Activity-related age indicators: (Chromospheric emission, X-Rays, Li, rotation)

Sydney A. Barnes
Leibniz Institute for Astrophysics Potsdam (AIP)
+ University of Potsdam, Germany
+ Space Science Institute, Boulder, USA

Context and reminders

- Age = diff. in time (measured with a suitable clock) between two events: birth, and present
- **Not an observable**; it must be deduced
- Multiple clocks necessary (availability of suitable data, ease of use, reliability, completeness, ...)
- Useful **only** if different clocks give the **same** age
- Activity-related indicators: Chromospheric emission (+X-Rays), rotation, Lithium, ...

Chromospheric Emission 1

Wilson, 1963

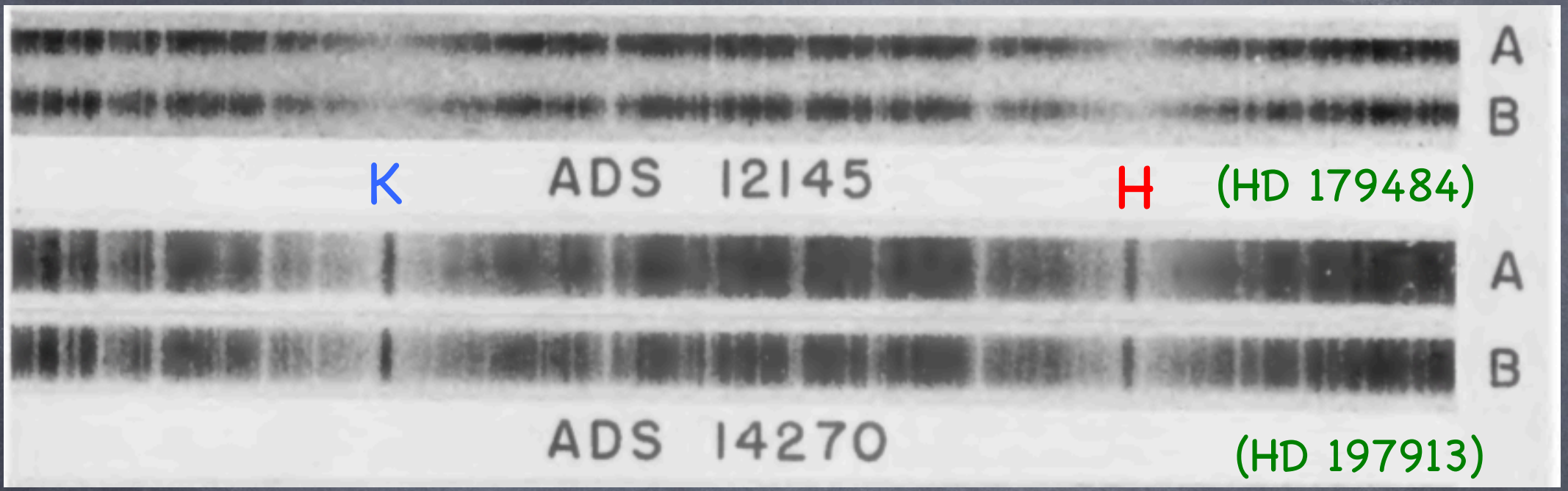

A PROBABLE CORRELATION BETWEEN CHROMOSPHERIC ACTIVITY AND AGE IN MAIN-SEQUENCE STARS

O. C. Wilson
Mount Wilson and Palomar Observatories
Carnegie Institution of Washington, California Institute of Technology
Received March 18, 1963

Benchmarks?

ABSTRACT

Observation shows that the average intensity of H and K emission is much higher for main-sequence stars of types G0–K2 in the Hyades, Praesepe, Coma, and Pleiades clusters than for similar local field stars and that it is appreciably higher for the Pleiades than for the other clusters. It is also found, from observations of local visual binaries, that the H-K intensities in the members of such pairs tend to be very similar when allowance is made for spectral-type differences. It is concluded that the most probable explanation of these facts is that the H-K intensity in a main-sequence star and hence the general degree of its chromospheric activity bear an inverse relationship to its age. This concept of chromospheric evolution is consistent with all the observations presented here, as well as with the known kinematical differences between dMe and ordinary dM stars. If, however, stars can be formed in the general field, as well as in clusters, then the observed differences in chromospheric activity would be related to place of origin rather than to age. The probable bearing of average surface magnetic-field strength on the question of chromospheric activity is discussed briefly.

Initially quantified by Skumanich 1972

Developed further by:
Noyes+1984,
Donahue 1998,
Soderblom+1991,
Wright+2004,
Mamajek+Hillenbrand 2008

Chromospheric Emission 2

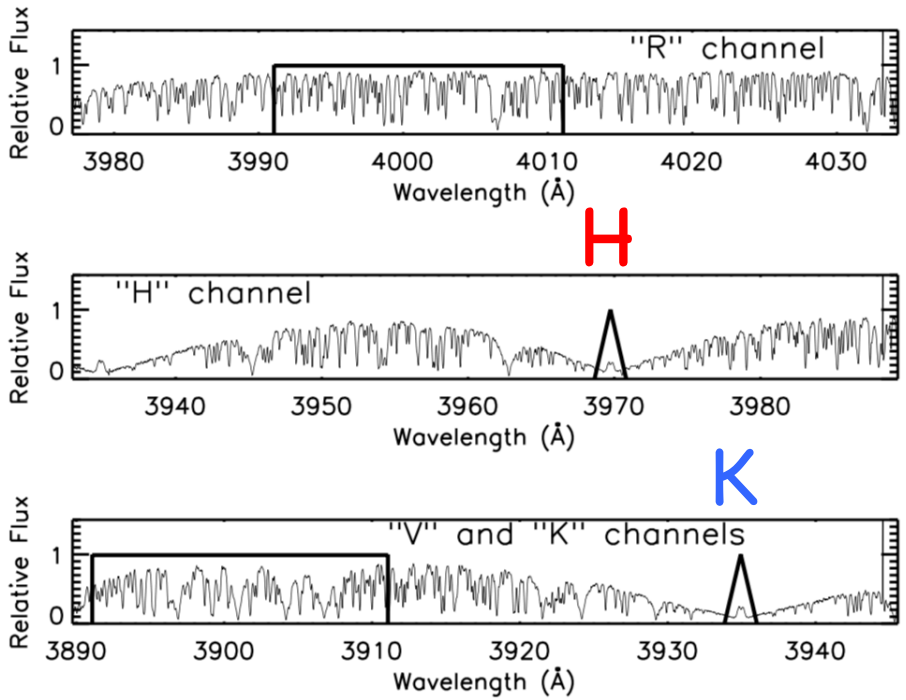

FIG. 1.—*R*, H, K, and *V* channels in a representative Keck spectrum. The ordinate is relative photon flux in arbitrary units. Wavelength is in the rest frame of the star. The H and K channels are always centered on the line cores; the *R* and *V* channels are fixed in the observer's frame.

$$S = \frac{aH + bK}{cR + dV}, \quad (3)$$

$$R_{HK} = 1.340 \times 10^{-4} C_{cf} S, \quad (9)$$

where

$$C_{cf}(B-V) = 1.13(B-V)^3 - 3.91(B-V)^2 + 2.84(B-V) - 0.47 \quad (10)$$

transforms the flux in the *R* and *V* channels to total continuum flux and *S* is the Mount Wilson *S*-value of the star. This number must be corrected for the photospheric contribution to the flux in the Ca II H and K line cores. Noyes et al. use the expression in Hartmann et al. (1984)

$$\log R_{phot} = -4.898 + 1.918(B-V)^2 - 2.893(B-V)^3 \quad (11)$$

to make the correction

$$R'_{HK} = R_{HK} - R_{phot}. \quad (12)$$

From these R'_{HK}-values one can derive rotation periods from the empirical fits of Noyes et al.:

$$\log(P_{rot}/\tau) = 0.324 - 0.400 \log R_5 - 0.283(\log R_5)^2 - 1.325(\log R_5)^3, \quad (13)$$

where R_5 is defined as $R'_{HK} \times 10^5$ and τ is the convective turnover time:

$$\log \tau = \begin{cases} 1.362 - 0.166x + 0.025x^2 - 5.323x^3, & x > 0, \\ 1.362 - 0.14x, & x < 0, \end{cases} \quad (14)$$

where $x = 1 - (B-V)$ and the ratio of mixing length to scale height is 1.9. Finally, we can calculate ages (Donahue 1993, cited in Henry et al. 1996):

$$\log t = 10.725 - 1.334R_5 + 0.4085R_5^2 - 0.0522R_5^3, \quad (15)$$

where *t* is the stellar age in years. The age calibration is cer-

R'_hk = R'_hk (t)

=> t = t (R'_hk)

Noyes+1984, Soderblom+1991, **Wright+2004**, Mamajek+Hillenbrand2008

Chromospheric Emission 3

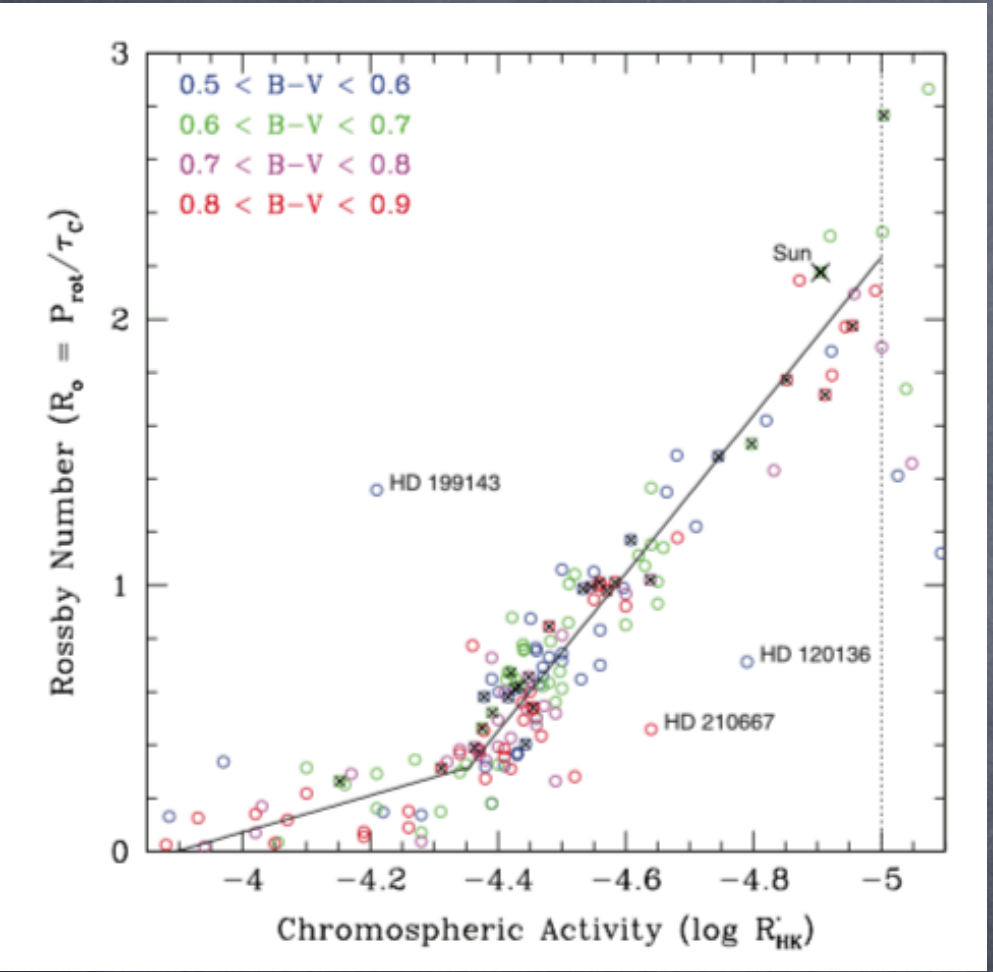

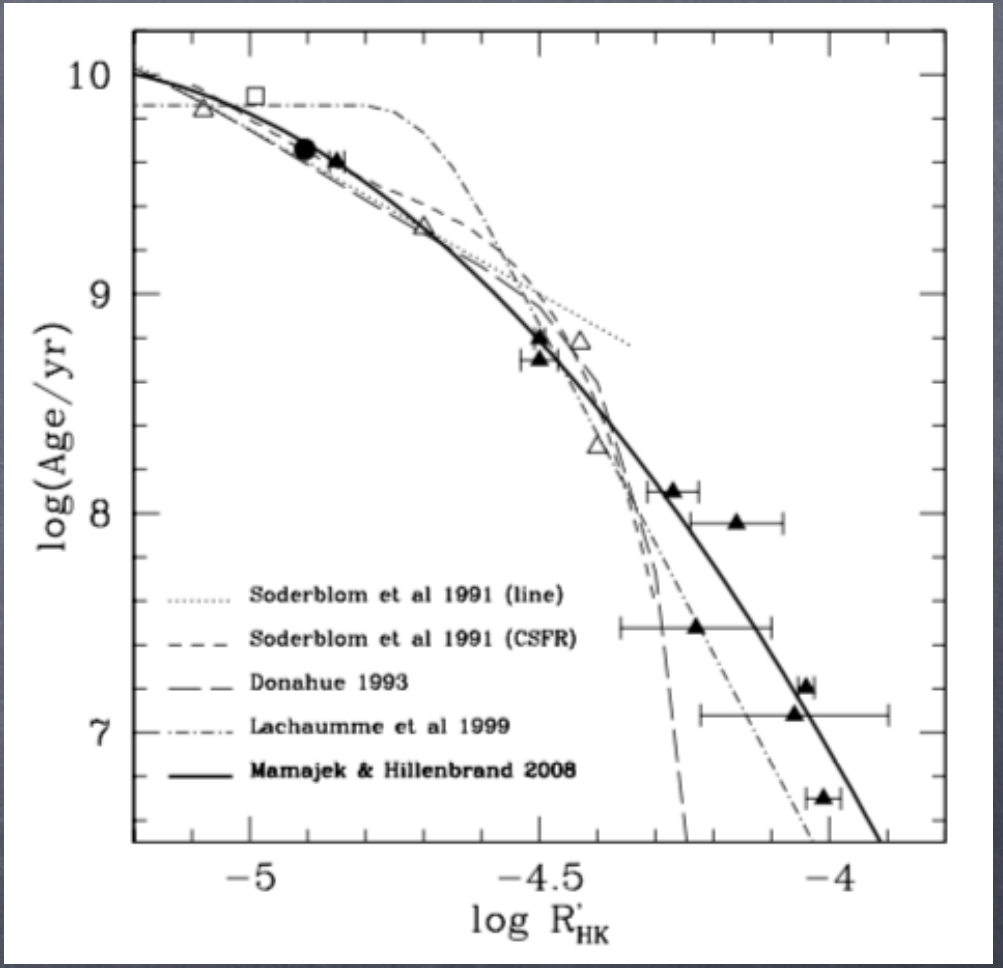

Noyes+1984, Soderblom+1991, Wright+2004, **Mamajek+Hillenbrand2008**

Chromospheric Emission 4

Wide binaries

Open clusters

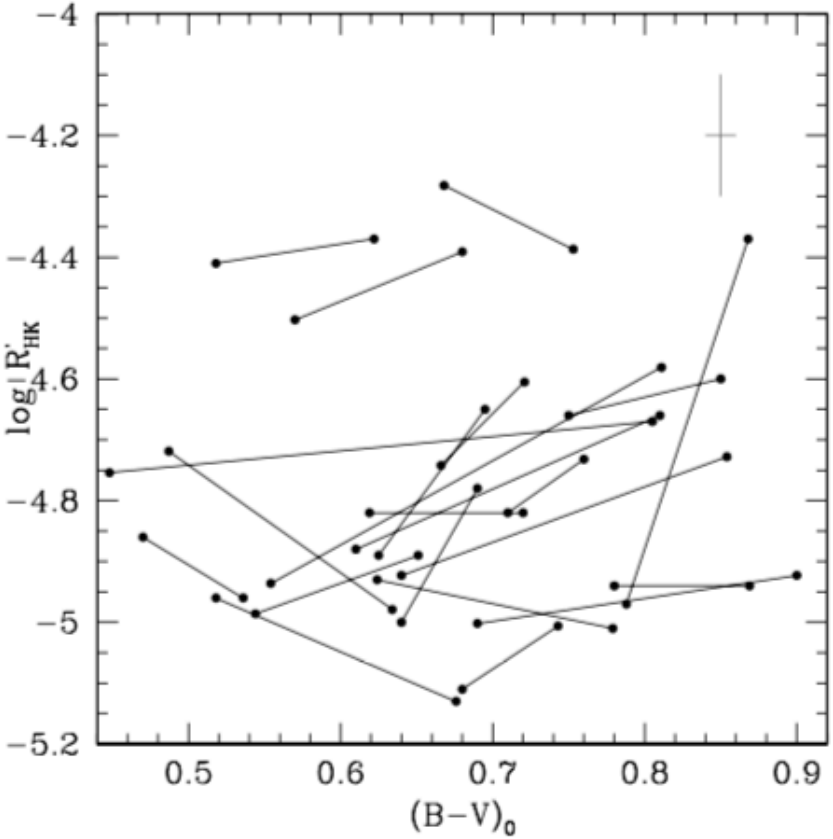

FIG. 3.—Color vs. activity for 23 nonidentical [$\Delta(B-V) \geq 0.05$] stellar binaries (see § 3.1.1). A typical error bar for $(B-V)$ colors (±0.01 mag) and for a single $\log R'_{HK}$ observation (±0.1 dex) is illustrated by the cross. The pair on the right side with the large slope is the pathological binary HD 137763.

Robinson 1992) and that the mean slope is $\overline{m} = 0.51 \pm 0.29$.

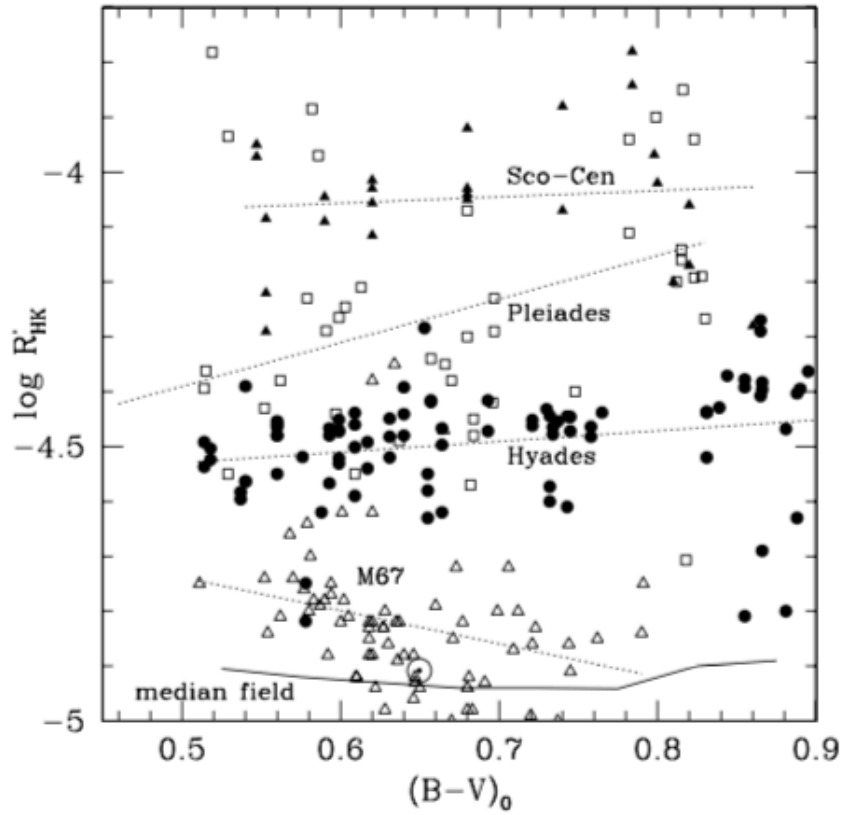

FIG. 4.—$(B-V)_0$ vs. $\log R'_{HK}$ for members of several stellar clusters in Table 5. Filled triangles are ~5–16 Myr Sco-Cen members (including Upper Sco, β Pic, UCL, LCC), open squares are ~130 Myr old Pleiades stars, filled circles are ~625 Myr old Hyades stars, and open triangles are ~4 Gyr old M67 members. Linear fits to the cluster data are shown by dashed lines. The circled dot is the Sun. The solid line represents the median $\log R'_{HK}$ for solar-type field stars (median $\log R'_{HK}$ values for 8 color bins from a sample of 1572 unique stars in the activity surveys of Henry et al. [1996] and Wright et al. [2004]).

Mamajek+Hillenbrand2008

X-Ray Emission

(More ->Talk by Stefanie Raetz)

R_x == L_x/L_bol; R_x = R_x (Ro) => t_x = t_x (Ro); Ro = P/tau

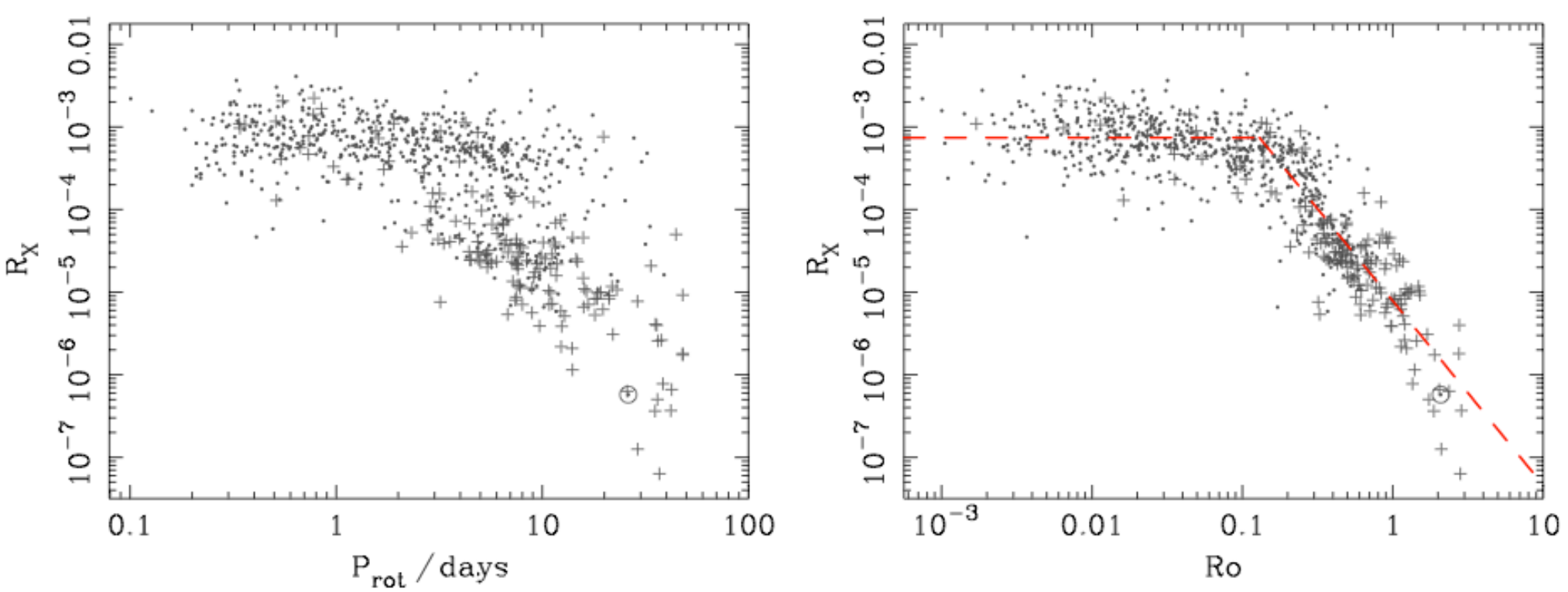

Figure 2. X-ray to bolometric luminosity ratio plotted against rotation period (left panel) and the Rossby number, Ro = P_{rot}/τ (right panel), for all stars in our sample with X-ray luminosities and photometric rotation periods. Stars known to be binaries are shown as plus symbols, and the Sun is indicated with a solar symbol. The best-fitting saturated and non-saturated activity–rotation relations described in the text are shown as a dashed red line in the right-hand panel.

(A color version of this figure is available in the online journal.)

Stauffer+1994, Patten+Simon1996, Pizzolato+2003, N J Wright+2011

Lithium

EW (Li) = EW (m, t)

Cummings+ 2017,
Soderblom 1993, 1995, 2010,
Sestito + Randich 2005
Chaboyer+1995
Deliyannis 2000, Jeffries 2000

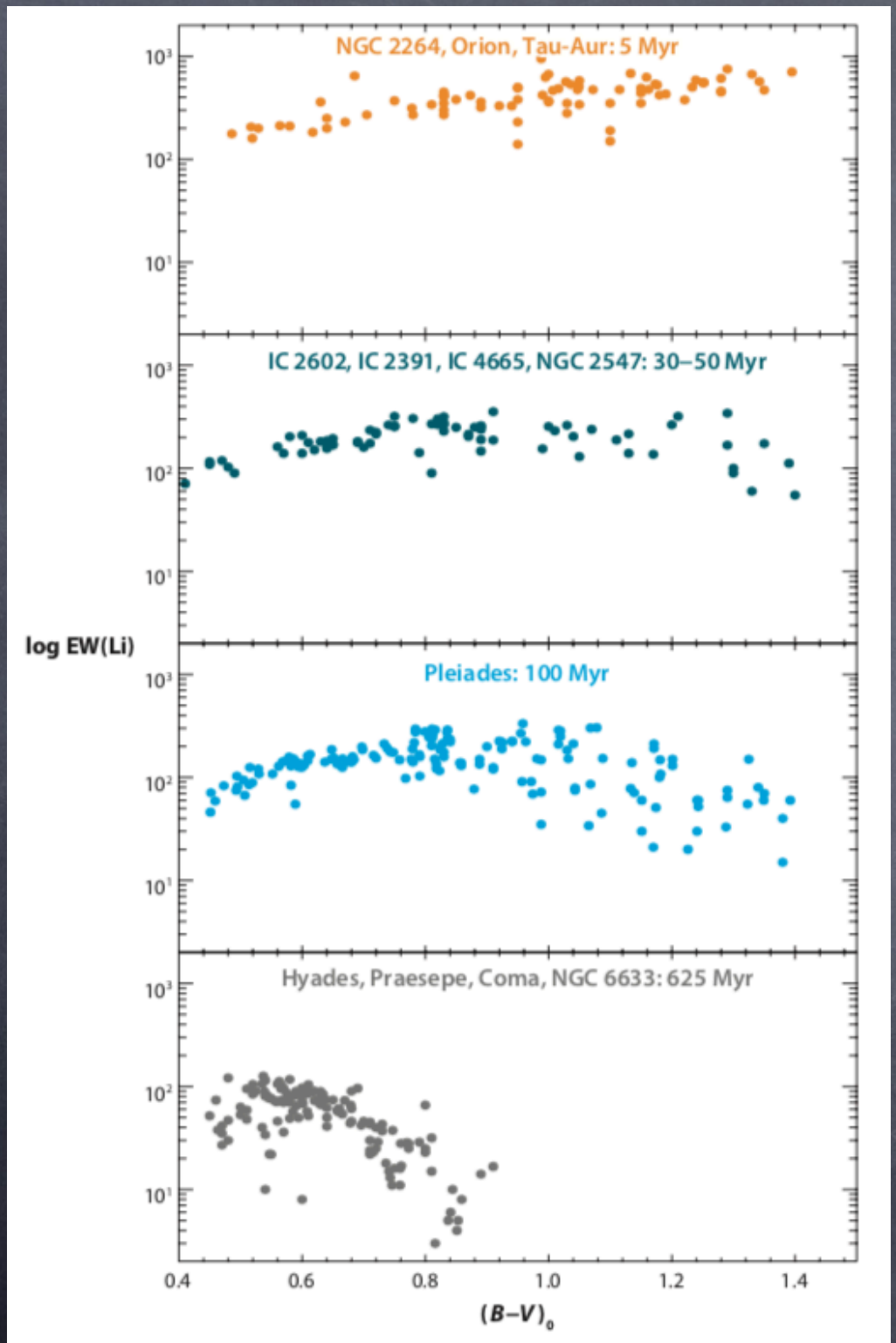

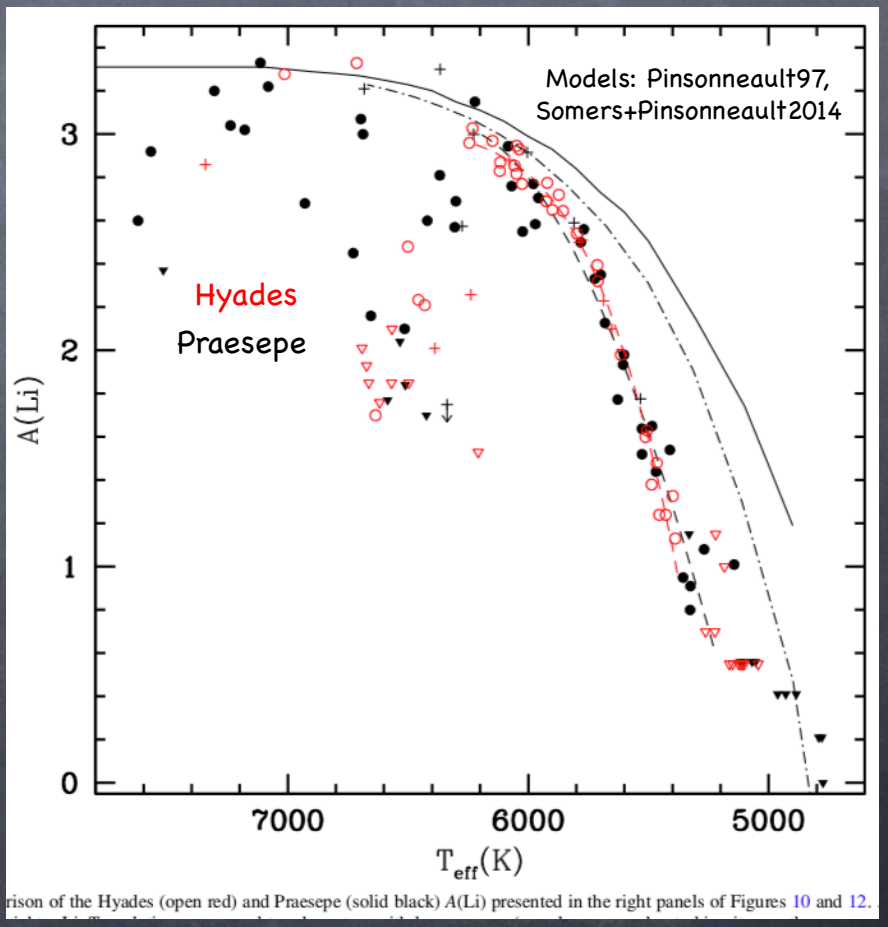

rison of the Hyades (open red) and Praesepe (solid black) A(Li) presented in the right panels of Figures 10 and 12.

Rotational Ages (gyrochronology)

P \propto Age (Sku72), but there is a color/mass dependence

Open cluster stars (younger)

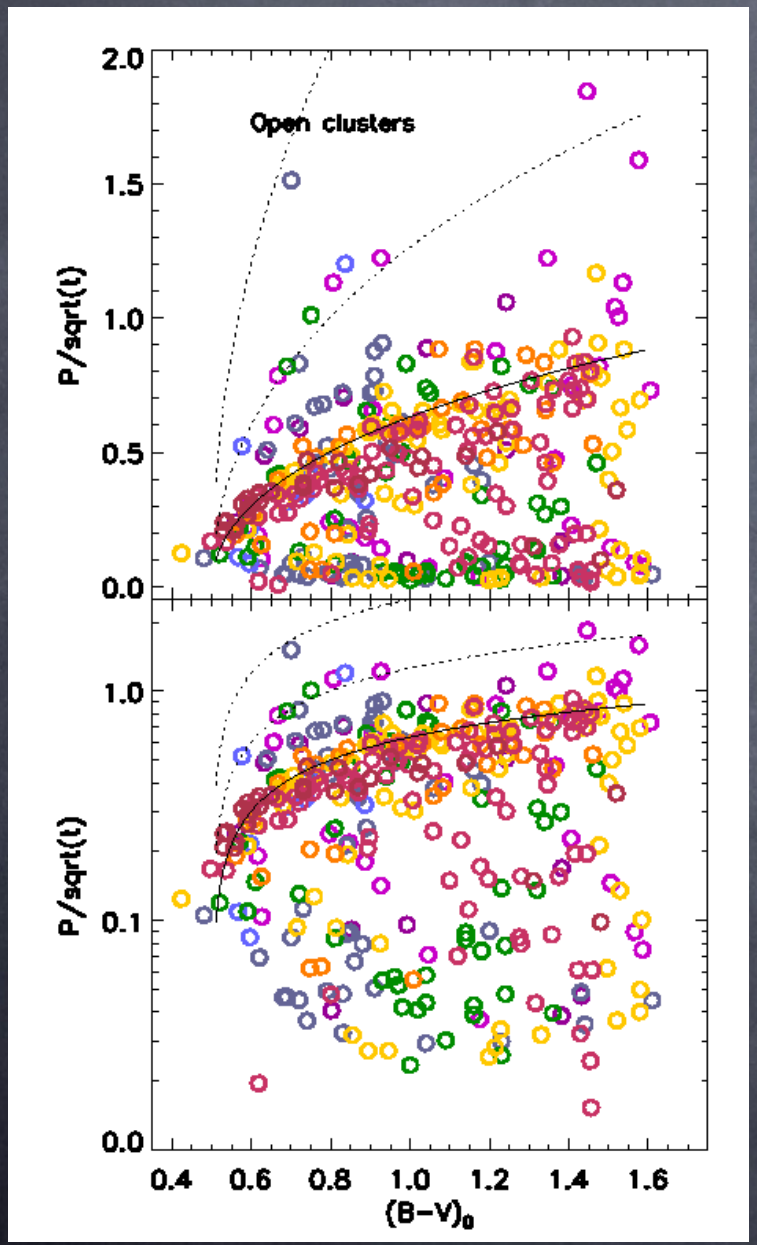

Field stars (older)

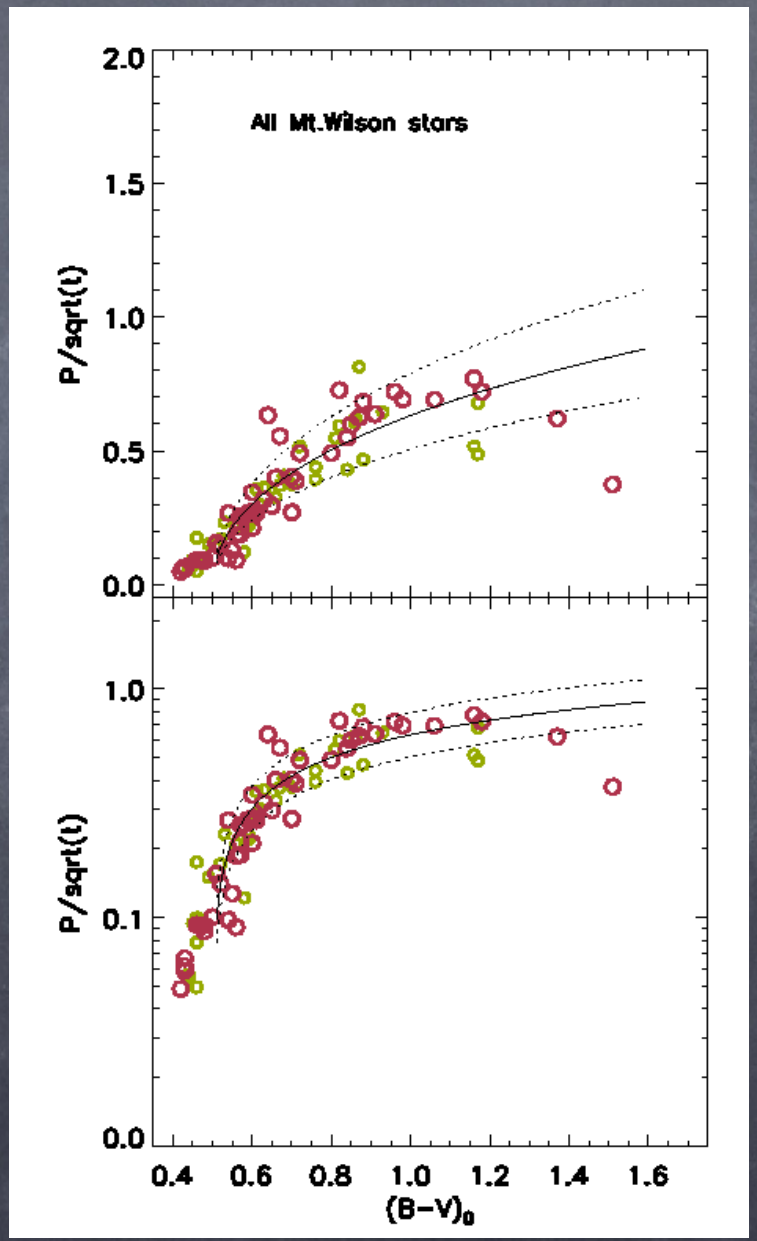

B03a, B07, Mamajek+ Hillenbrand2008, Meibom+2011, Angus+2015

Gyrochronology

Slow rotators spin down Skumanich-style

B07

$$P_I(B-V,t) = f(B-V).g(t)$$

$$g(t) = \sqrt{t}$$

$$f(B-V) = a(B-V-c)^b$$

$$a,b,c = 0.778,0.519,0.4$$

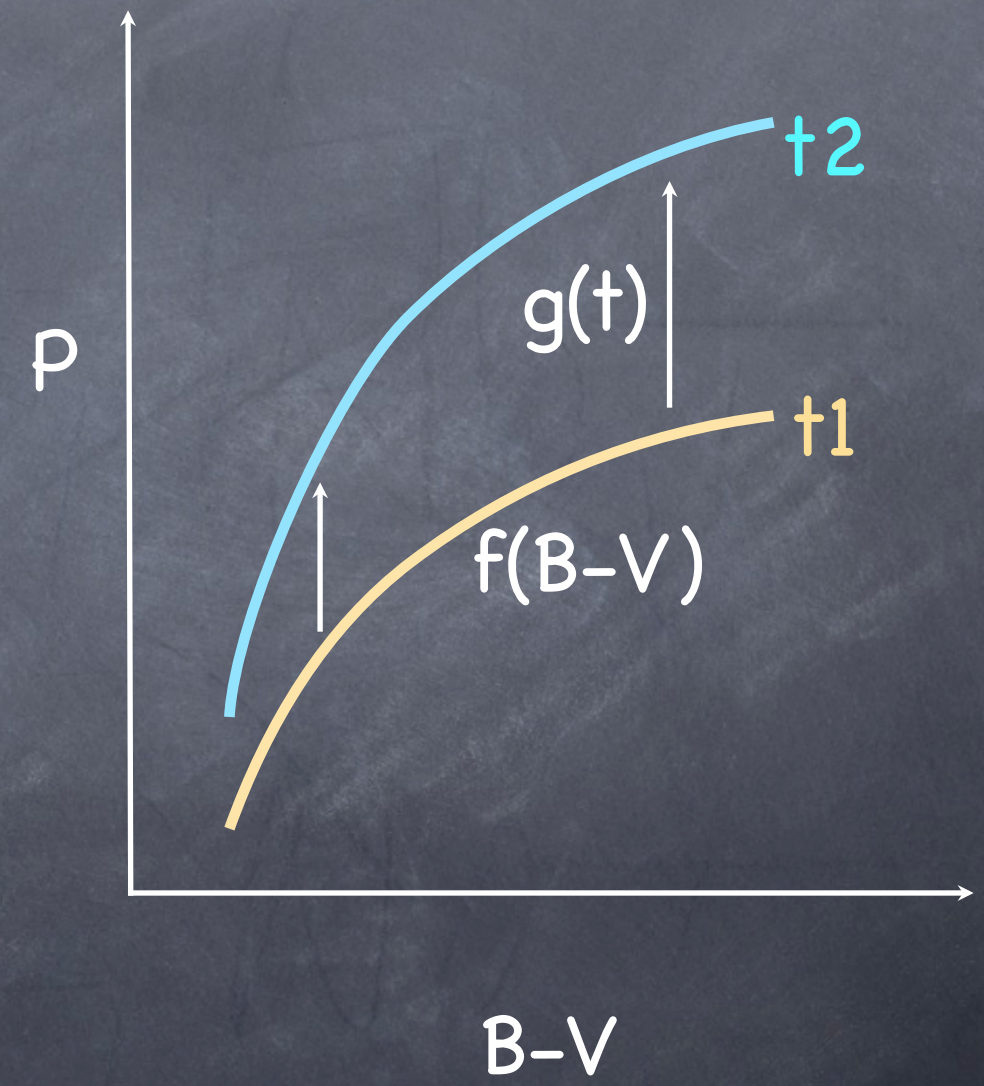

Gyrochronology

Progress in observations...

Meibom+2009 (M35)

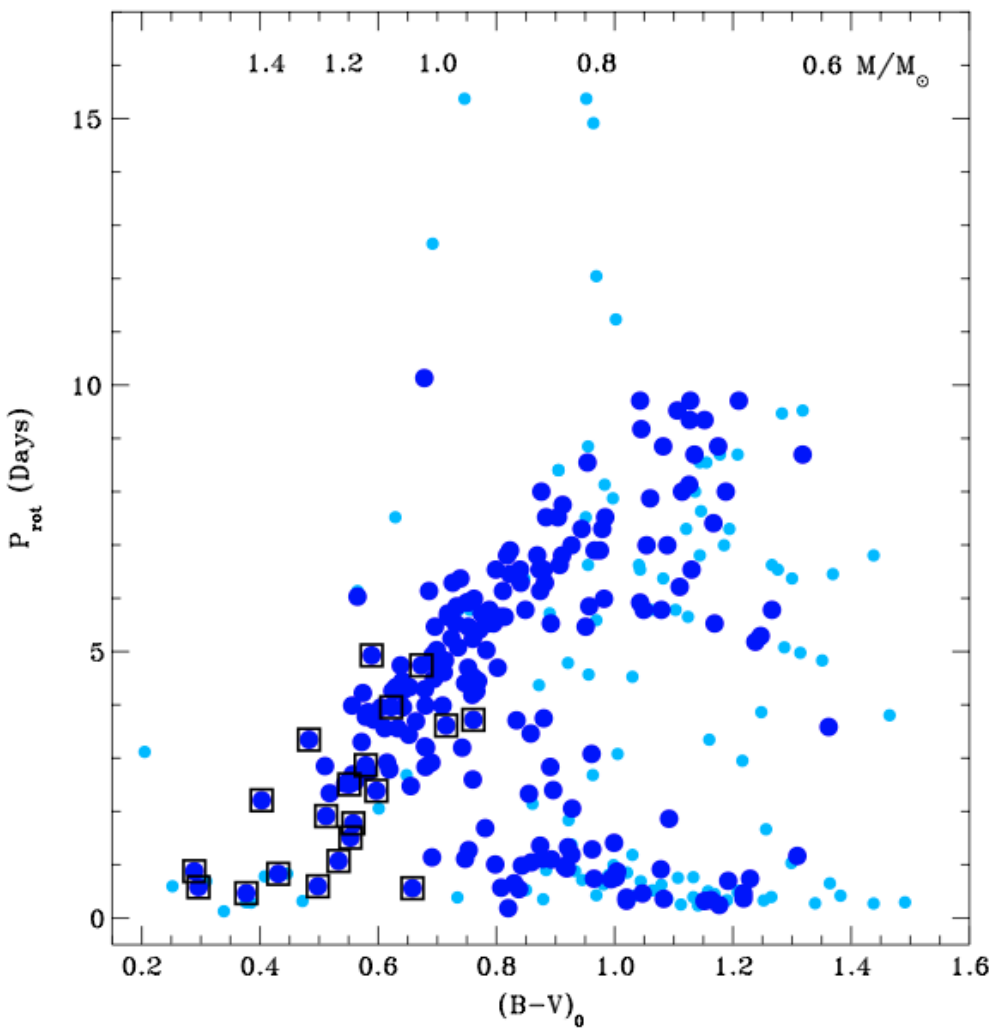

M34

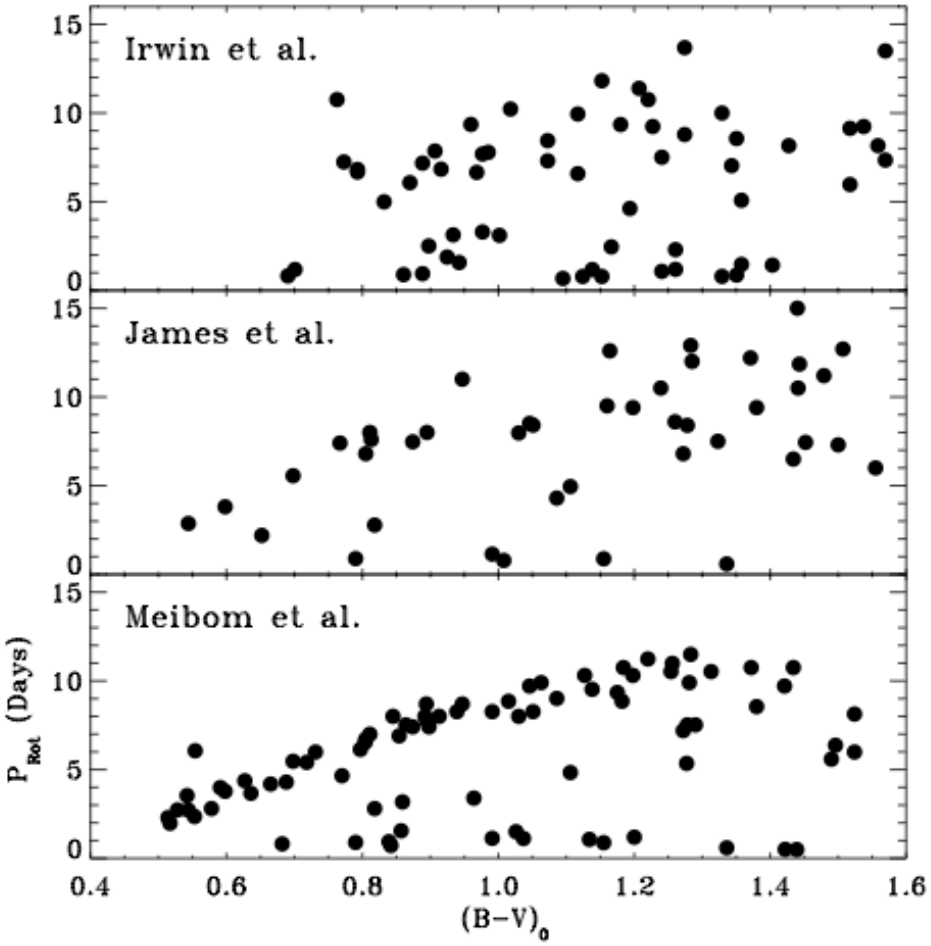

Figure 8. Color–period diagrams based on the results from Irwin et al. (2006, top), James et al. (2010, center), and from the present study (bottom).

Gyrochronology

Progress in theory...

Pre-2010 (separable) models
B03, B07, Mamajek+Hill2008, Meibom2011, Angus+2015

B10 model (dP/dt = fn of Ro);
c.f. Brown 2014, Matt+2015, Amard+2016

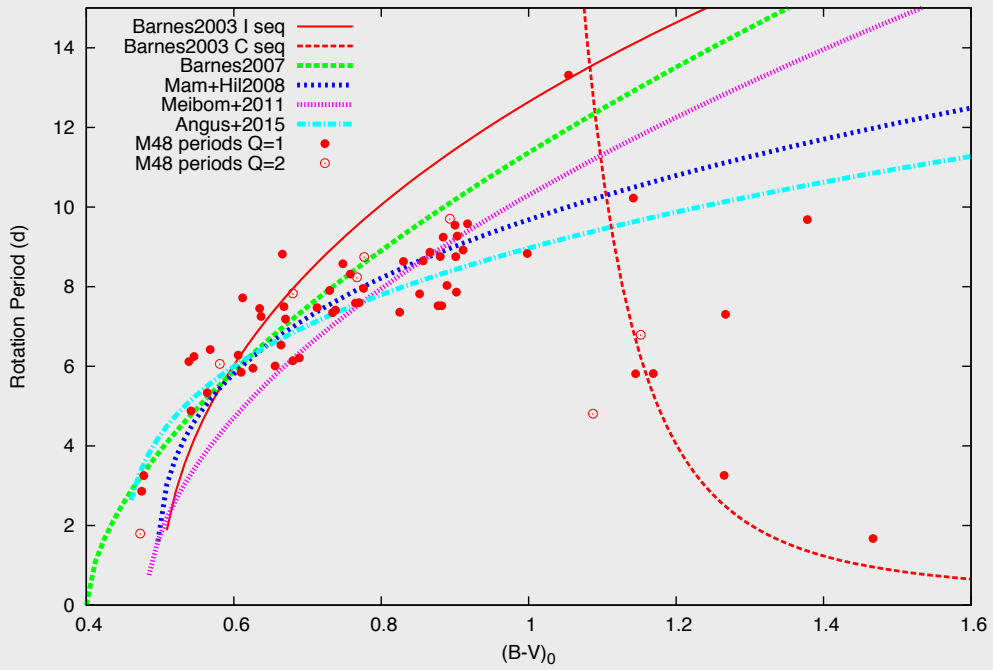

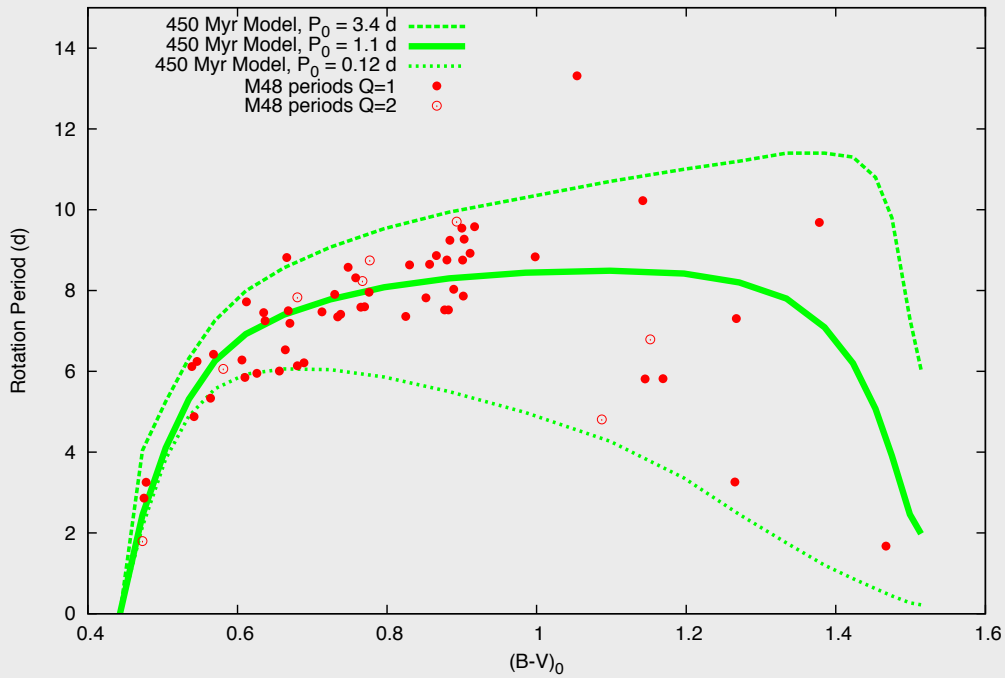

But we already know of trouble w. younger clusters...

For Ro = P/tau, can get tau from B+Kim2010

(Other tau values similar, but need to recalibrate 2 constants)

Table 1

Calculated Properties of Solar Metallicity Main-sequence Stellar Models at 500 Myr, as Used in the Text

Mass	log T	log $L/L_\odot$	Age	Global τ_c	Local τ_c	Moment of Inertia (g cm^2)				Lejeune et al. (1997, 1998) Colors							
($M_\odot$)	(K)	-	(Gyr)	(d)	(d)	Con. Core	Rad. Zone	Con. Env	Total	*U*	*B*	*V*	*R*	*I*	*J*	*H*	*K*
0.15	3.50961	−2.53866	0.500	3.398*e* + 02	1.628*e* + 02	0.000*e* + 00	0.000*e* + 00	8.922*e* + 51	8.922*e* + 51	16.391	15.056	13.425	12.221	10.701	9.254	8.640	8.385
0.20	3.52474	−2.28585	0.500	3.679*e* + 02	1.784*e* + 02	0.000*e* + 00	0.000*e* + 00	1.839*e* + 52	1.839*e* + 52	15.172	14.000	12.464	11.357	9.986	8.666	8.041	7.805
0.25	3.53505	−2.10378	0.500	4.086*e* + 02	2.030*e* + 02	0.000*e* + 00	0.000*e* + 00	3.166*e* + 52	3.166*e* + 52	14.472	13.316	11.788	10.719	9.484	8.282	7.652	7.432
0.30	3.54339	−1.95807	0.500	4.930*e* + 02	2.565*e* + 02	0.000*e* + 00	0.000*e* + 00	4.907*e* + 52	4.907*e* + 52	13.896	12.761	11.247	10.214	9.089	7.976	7.339	7.133
0.35	3.55082	−1.81901	0.500	3.584*e* + 02	1.718*e* + 02	1.330*e* + 51	2.140*e* + 51	6.991*e* + 52	7.338*e* + 52	13.457	12.308	10.809	9.802	8.729	7.641	7.006	6.806
0.40	3.55929	−1.69122	0.500	2.221*e* + 02	1.133*e* + 02	7.920*e* + 50	2.080 + 52	7.952*e* + 52	1.011*e* + 53	13.042	11.873	10.398	9.422	8.402	7.332	6.694	6.503
0.45	3.56950	−1.55867	0.500	1.769*e* + 02	9.196*e* + 01	7.784*e* + 50	4.435*e* + 52	8.833*e* + 52	1.334*e* + 53	12.600	11.402	9.949	9.008	8.056	7.014	6.377	6.195
0.50	3.58154	−1.42169	0.500	1.468*e* + 02	7.728*e* + 01	6.085*e* + 50	7.457*e* + 52	9.507*e* + 52	1.702*e* + 53	12.117	10.895	9.472	8.566	7.680	6.705	6.065	5.897
0.55	3.59551	−1.28094	0.500	1.254*e* + 02	6.612*e* + 01	3.030*e* + 50	1.117*e* + 53	9.931*e* + 52	2.114*e* + 53	11.582	10.343	8.958	8.086	7.270	6.406	5.769	5.617
0.60	3.61129	−1.13877	0.500	1.068*e* + 02	5.729*e* + 01	6.108*e* + 49	1.517*e* + 53	1.044*e* + 53	2.562*e* + 53	11.029	9.789	8.455	7.638	6.905	6.080	5.443	5.312
0.65	3.62846	−0.99758	0.500	9.305*e* + 01	5.012*e* + 01	0.000*e* + 00	1.969*e* + 53	1.070*e* + 53	3.038*e* + 53	10.439	9.230	7.959	7.217	6.580	5.736	5.113	5.002
0.70	3.64654	−0.85948	0.500	8.117*e* + 01	4.400*e* + 01	0.000*e* + 00	2.454*e* + 53	1.082*e* + 53	3.536*e* + 53	9.832	8.696	7.499	6.819	6.253	5.415	4.810	4.708
0.75	3.66575	−0.72461	0.500	7.089*e* + 01	3.887*e* + 01	0.000*e* + 00	2.954*e* + 53	1.090*e* + 53	4.044*e* + 53	9.124	8.120	7.022	6.420	5.926	5.123	4.555	4.459
0.80	3.68619	−0.59368	0.500	6.254*e* + 01	3.458*e* + 01	0.000*e* + 00	3.460*e* + 53	1.093*e* + 53	4.553*e* + 53	8.349	7.543	6.558	6.032	5.594	4.866	4.346	4.258
0.85	3.70568	−0.46899	0.500	5.501*e* + 01	3.079*e* + 01	0.000*e* + 00	3.994*e* + 53	1.081*e* + 53	5.074*e* + 53	7.634	7.040	6.157	5.681	5.270	4.632	4.153	4.074
0.90	3.72368	−0.35030	0.500	4.790*e* + 01	2.729*e* + 01	0.000*e* + 00	4.572*e* + 53	1.036*e* + 53	5.608*e* + 53	7.015	6.605	5.809	5.367	4.974	4.404	3.959	3.886
0.95	3.73984	−0.23755	0.500	4.124*e* + 01	2.400*e* + 01	0.000*e* + 00	5.191*e* + 53	9.679*e* + 52	6.159*e* + 53	6.475	6.204	5.480	5.070	4.695	4.191	3.790	3.723
1.00	3.75439	−0.12957	0.500	3.487*e* + 01	2.080*e* + 01	0.000*e* + 00	5.852*e* + 53	8.648*e* + 52	6.717*e* + 53	5.992	5.835	5.173	4.797	4.446	3.987	3.625	3.568
1.05	3.76739	−0.02597	0.500	2.864*e* + 01	1.757*e* + 01	0.000*e* + 00	6.570*e* + 53	7.092*e* + 52	7.279*e* + 53	5.583	5.499	4.888	4.541	4.213	3.779	3.446	3.394
1.10	3.77903	0.07324	0.500	2.193*e* + 01	1.419*e* + 01	4.481*e* + 50	7.310*e* + 53	5.254 + 52	7.840*e* + 53	5.226	5.190	4.620	4.298	3.992	3.573	3.263	3.212
1.15	3.78948	0.16746	0.500	1.467*e* + 01	1.069*e* + 01	1.960*e* + 51	8.049*e* + 53	3.331*e* + 52	8.401*e* + 53	4.911	4.898	4.363	4.061	3.774	3.392	3.107	3.060
1.20	3.79899	0.25725	0.500	8.141*e* + 00	7.440*e* + 00	3.944*e* + 51	8.770*e* + 53	1.525*e* + 52	8.962*e* + 53	4.617	4.623	4.119	3.837	3.566	3.218	2.959	2.916
1.25	3.80807	0.34281	0.500	2.394*e* + 00	0.000*e* + 00	5.794*e* + 51	9.448*e* + 53	2.806*e* + 51	9.534*e* + 53	4.344	4.363	3.890	3.625	3.371	3.056	2.822	2.782
1.30	3.81760	0.42605	0.500	0.000*e* + 00	0.000*e* + 00	6.669*e* + 51	1.004*e* + 54	0.000*e* + 00	1.010*e* + 54	4.084	4.110	3.667	3.420	3.182	2.902	2.694	2.657
1.35	3.82645	0.50530	0.500	0.000*e* + 00	0.000*e* + 00	7.989*e* + 51	1.065*e* + 54	0.000*e* + 00	1.073*e* + 54	3.848	3.873	3.457	3.226	3.001	2.754	2.570	2.535
1.40	3.83525	0.58081	0.500	0.000*e* + 00	0.000*e* + 00	9.578*e* + 51	1.132*e* + 54	0.000*e* + 00	1.141*e* + 54	3.623	3.648	3.260	3.048	2.838	2.613	2.448	2.415
1.45	3.84458	0.65226	0.500	0.000*e* + 00	0.000*e* + 00	1.106*e* + 52	1.206*e* + 54	0.000*e* + 00	1.218*e* + 54	3.404	3.432	3.076	2.885	2.693	2.483	2.337	2.306
1.50	3.85476	0.72048	0.500	0.000*e* + 00	0.000*e* + 00	1.331*e* + 52	1.288*e* + 54	0.000*e* + 00	1.302*e* + 54	3.227	3.227	2.896	2.721	2.539	2.366	2.232	2.201

Older clusters: NGC 6811 (1 Gyr)

Meibom+2011, 2013

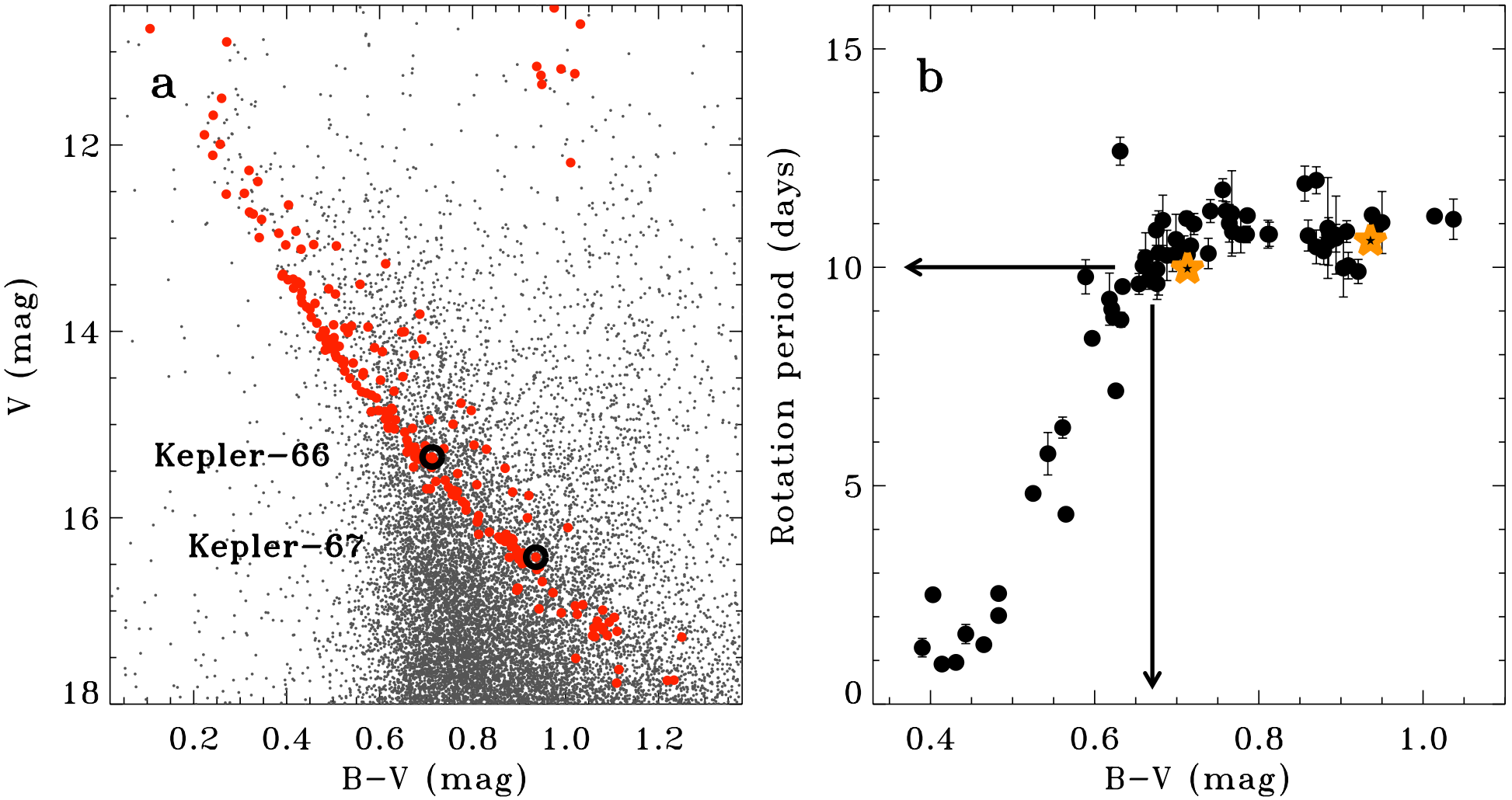

Older clusters: NGC 6819 (2.5 Gyr)

Meibom+ 2015

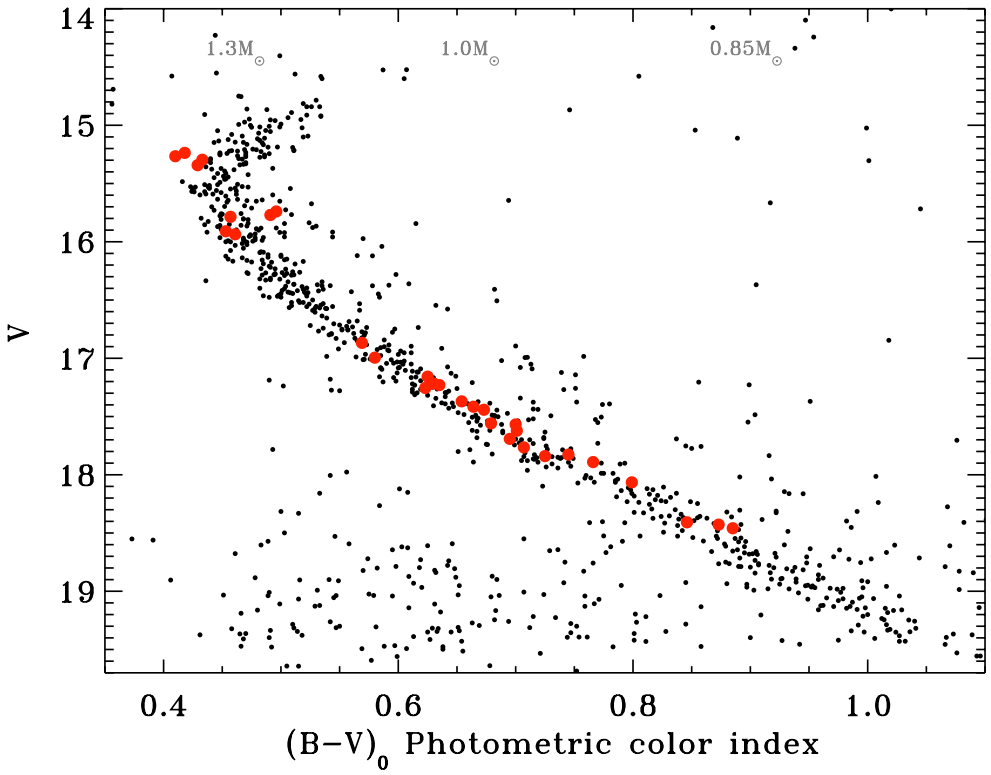

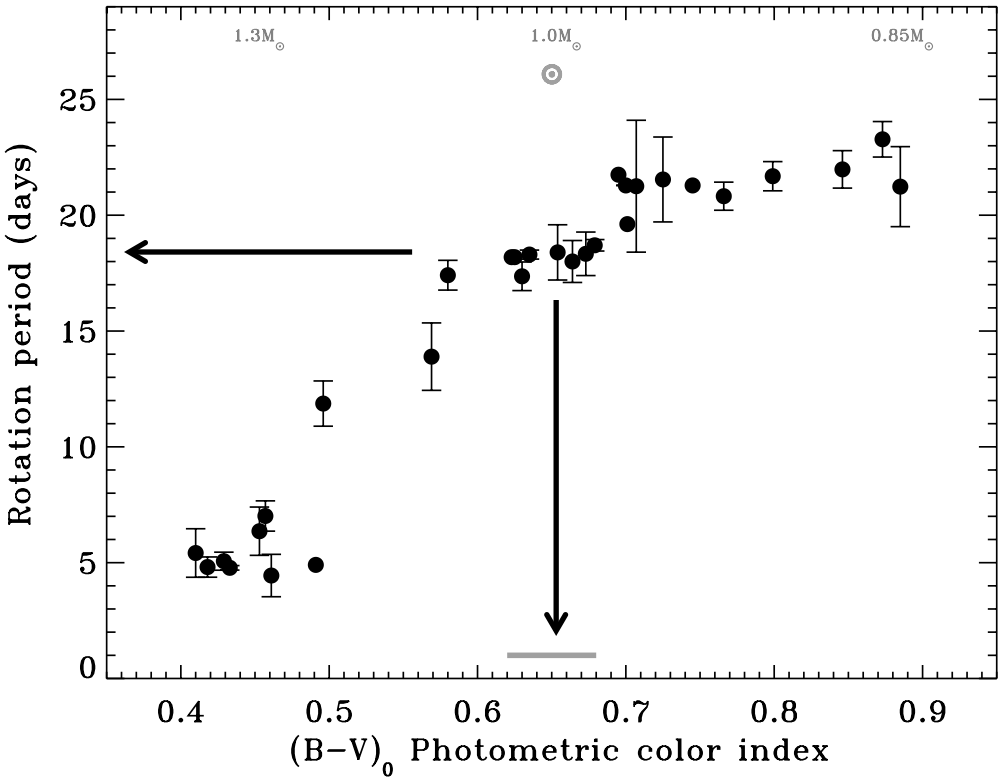

Older clusters: M67 (4.2 Gyr)

B+2016

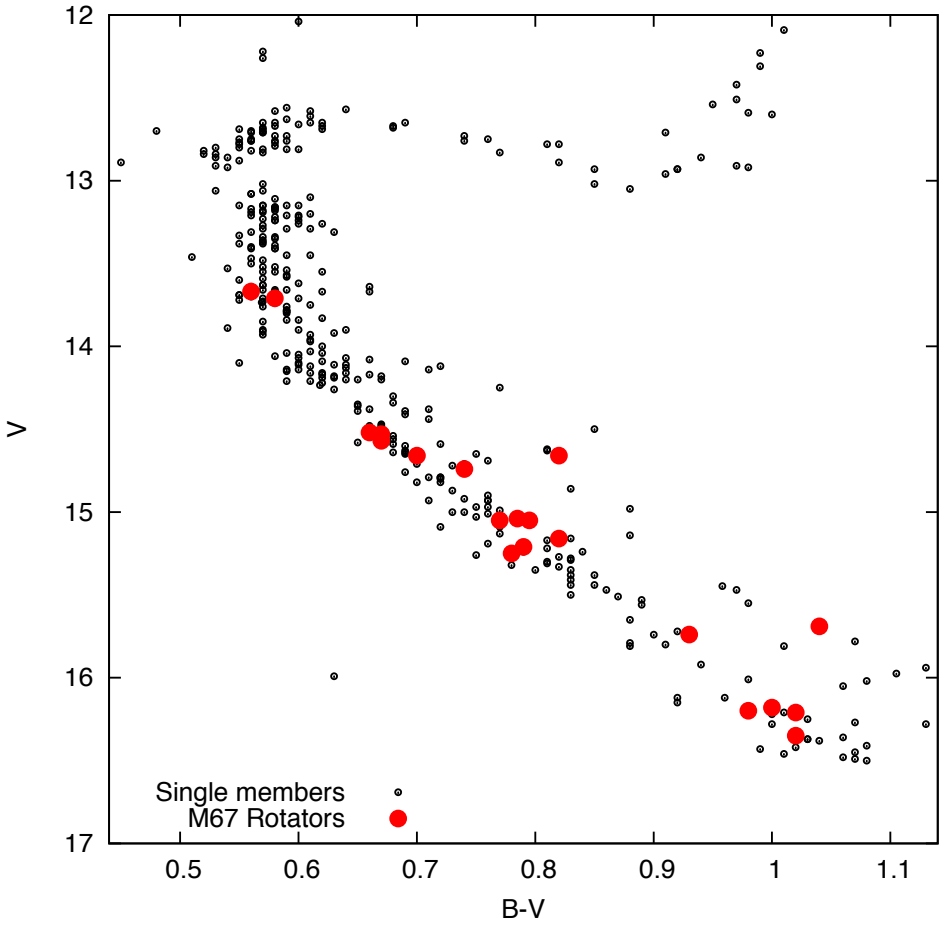

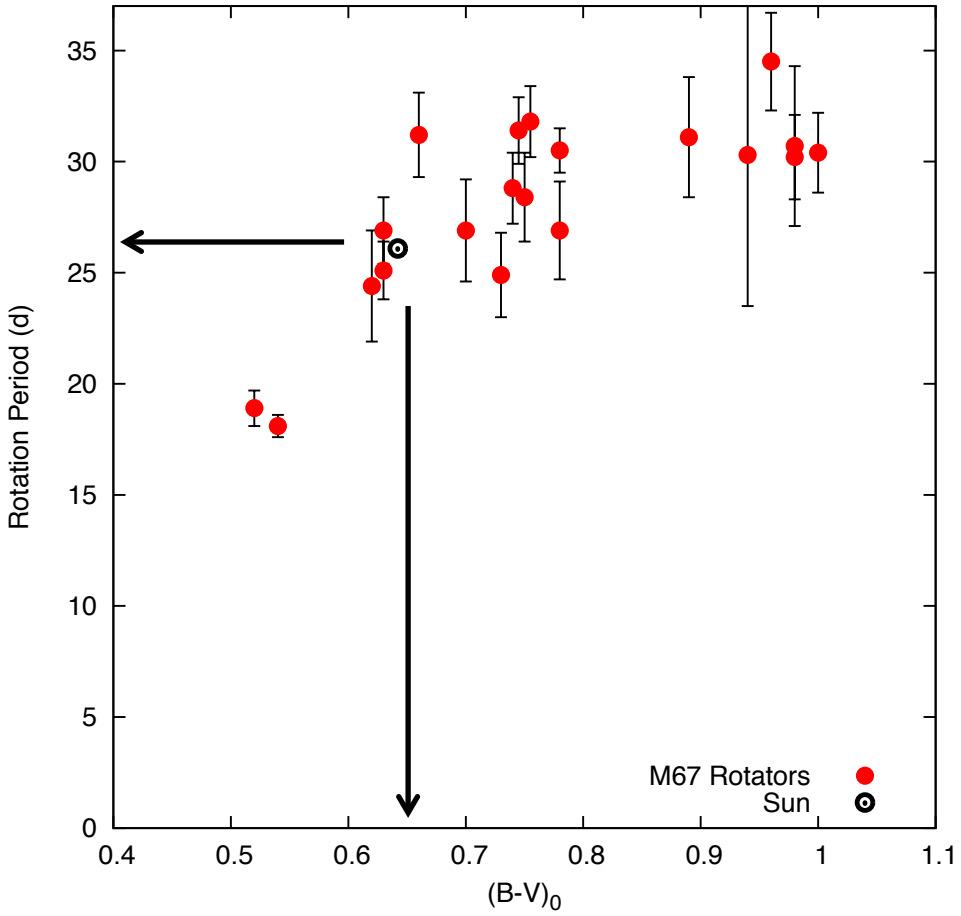

M67 (4.2 Gyr)

B+2016

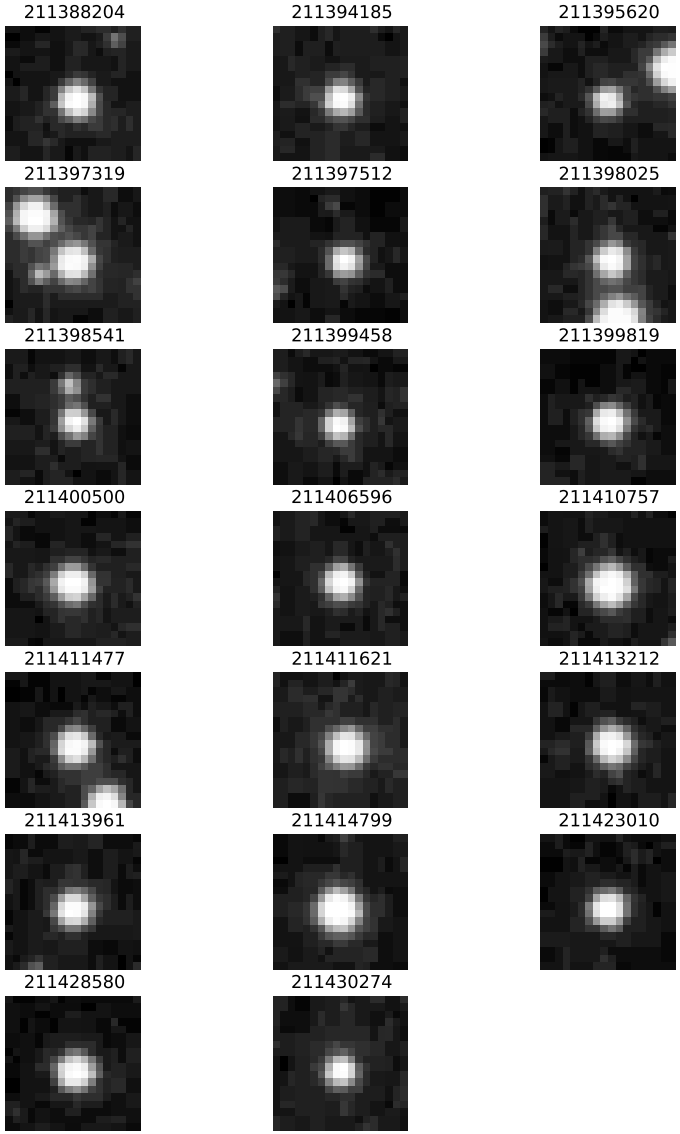

4 arcsec pixels!

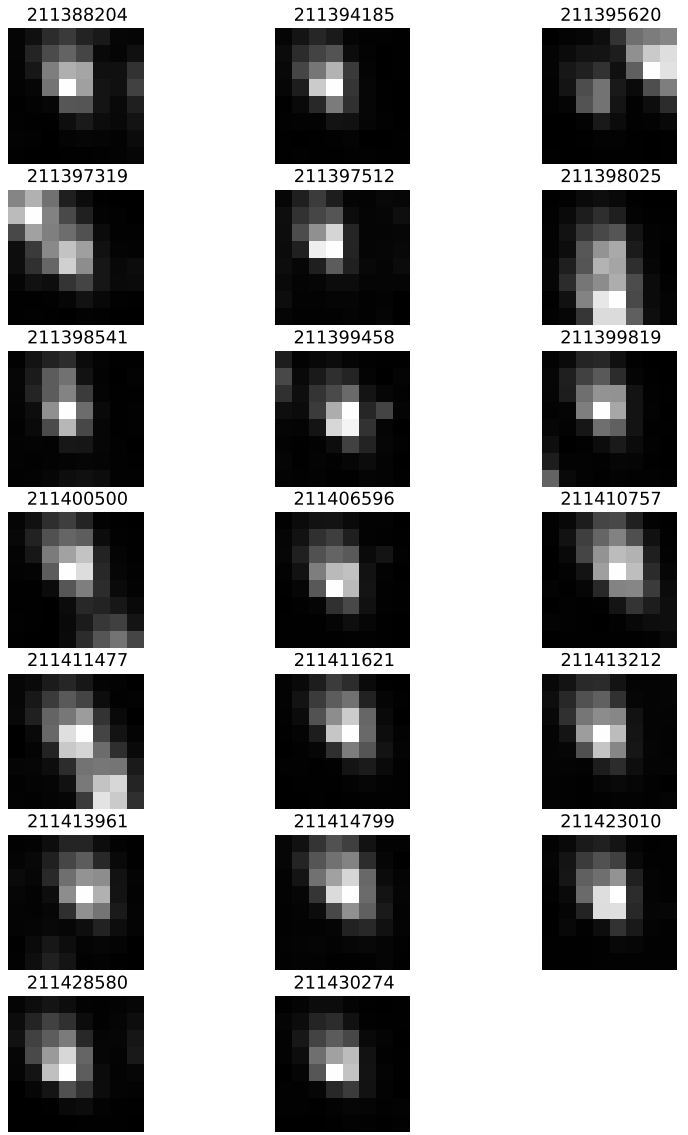

M67 (4.2 Gyr)

= Joerg Weingrill

B+2016

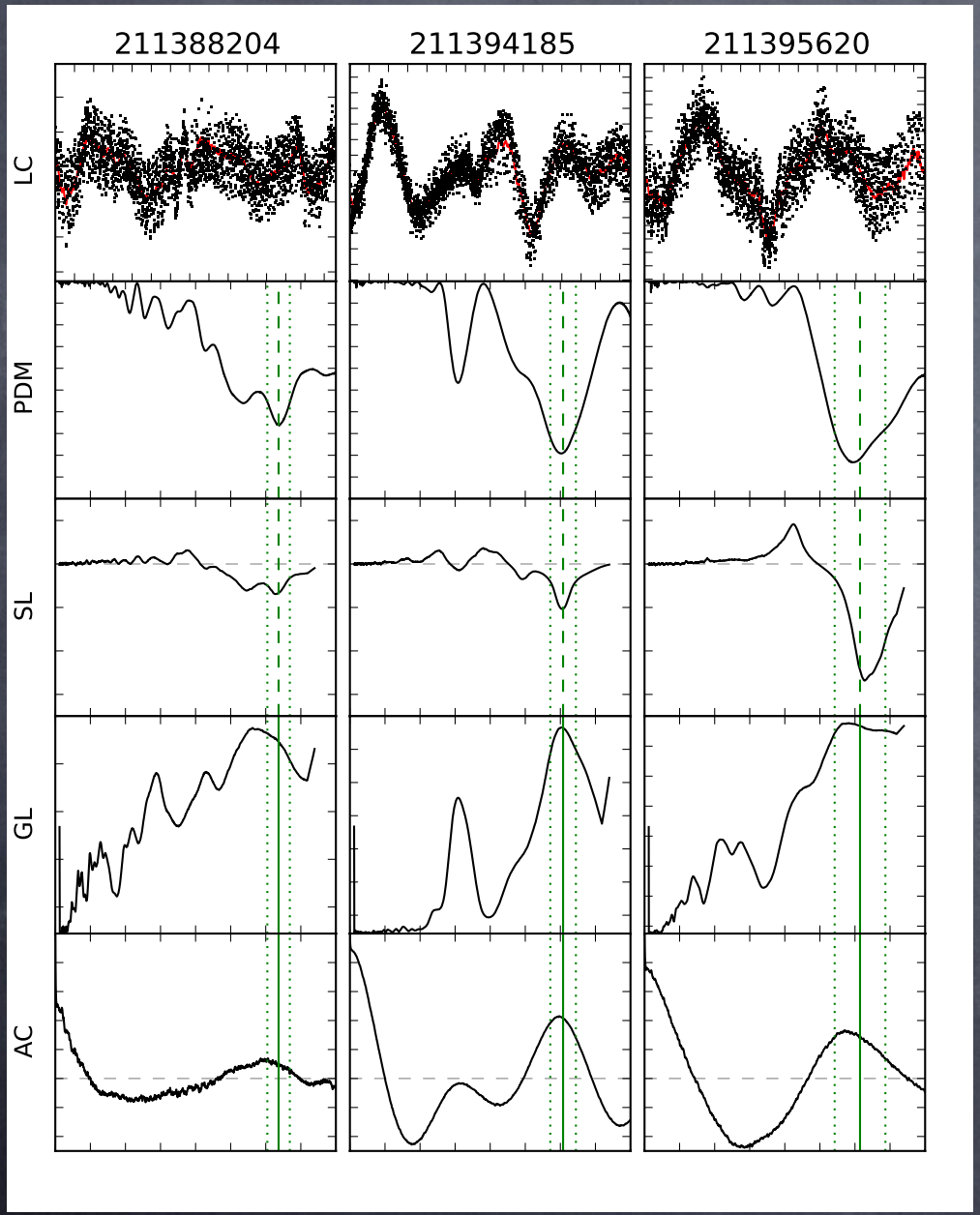

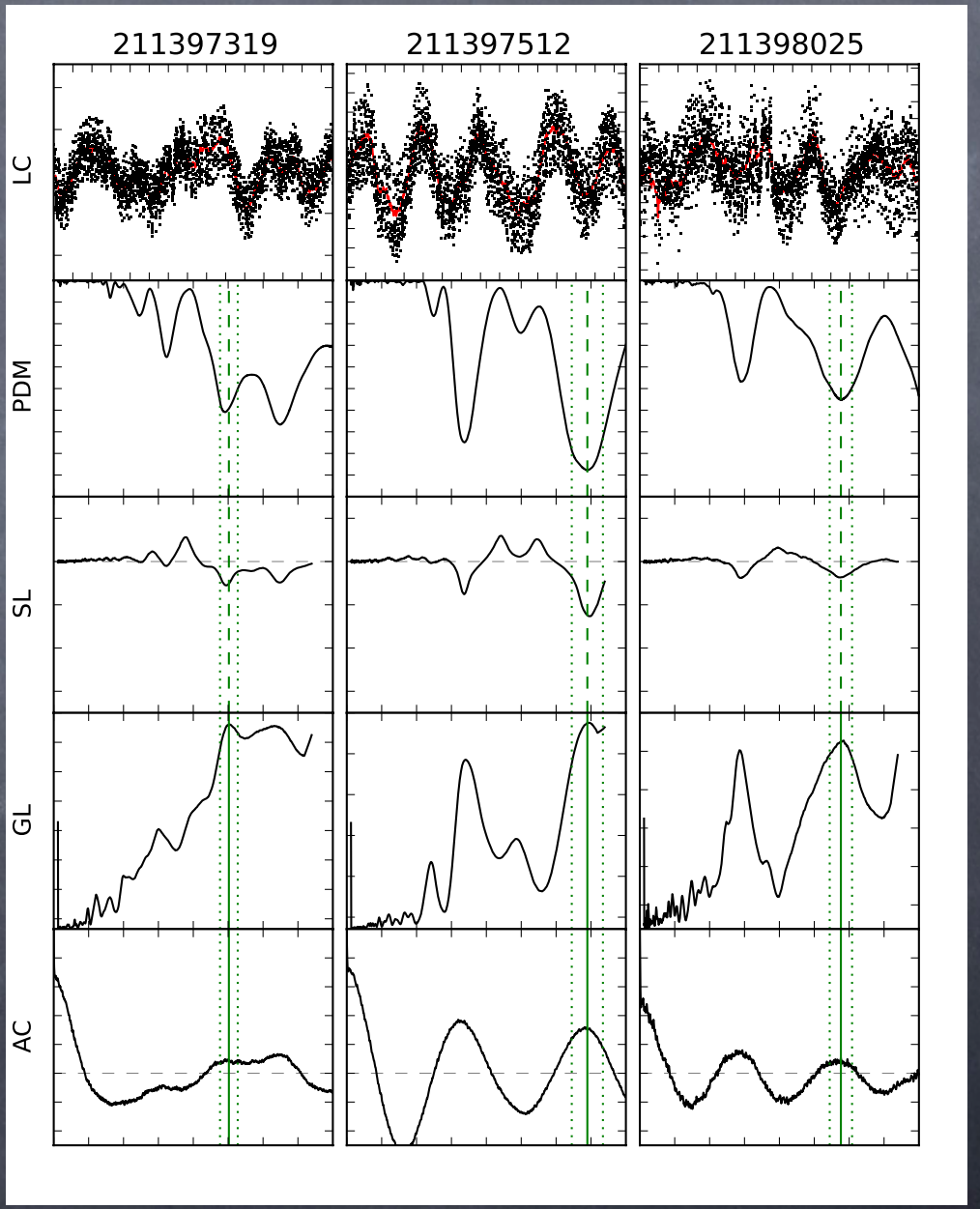

M67 compared with models, Sun, and prior clusters

B+2016

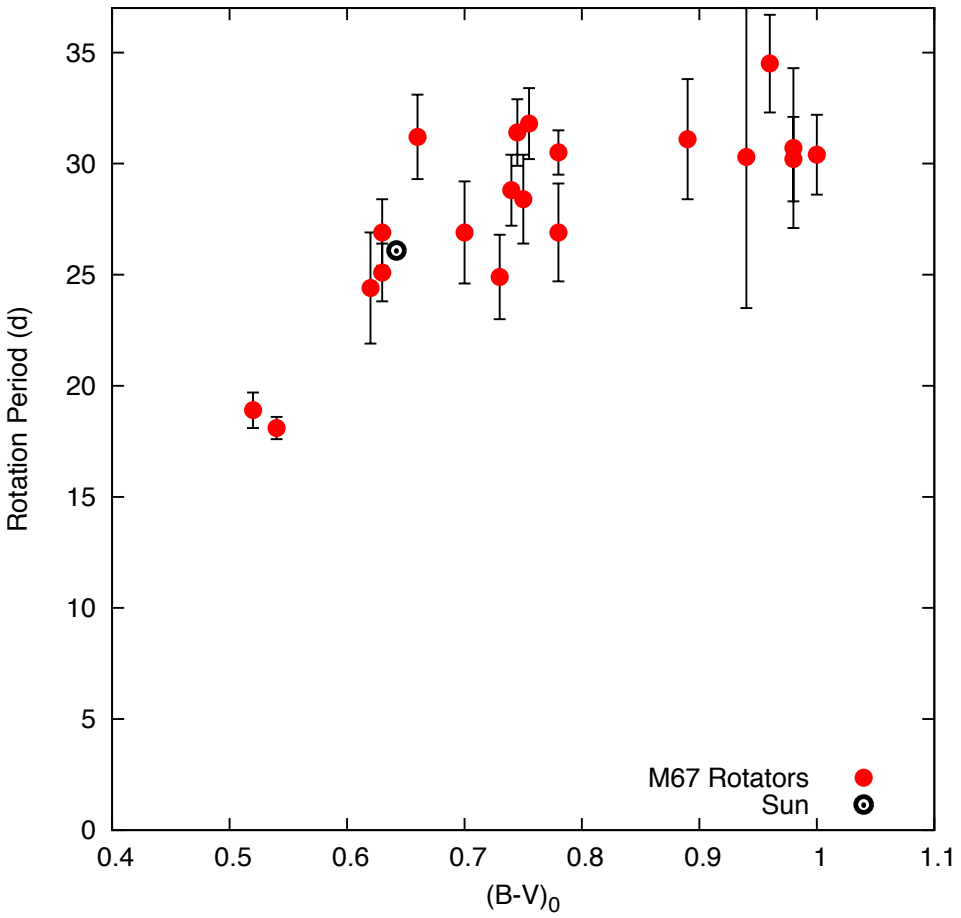

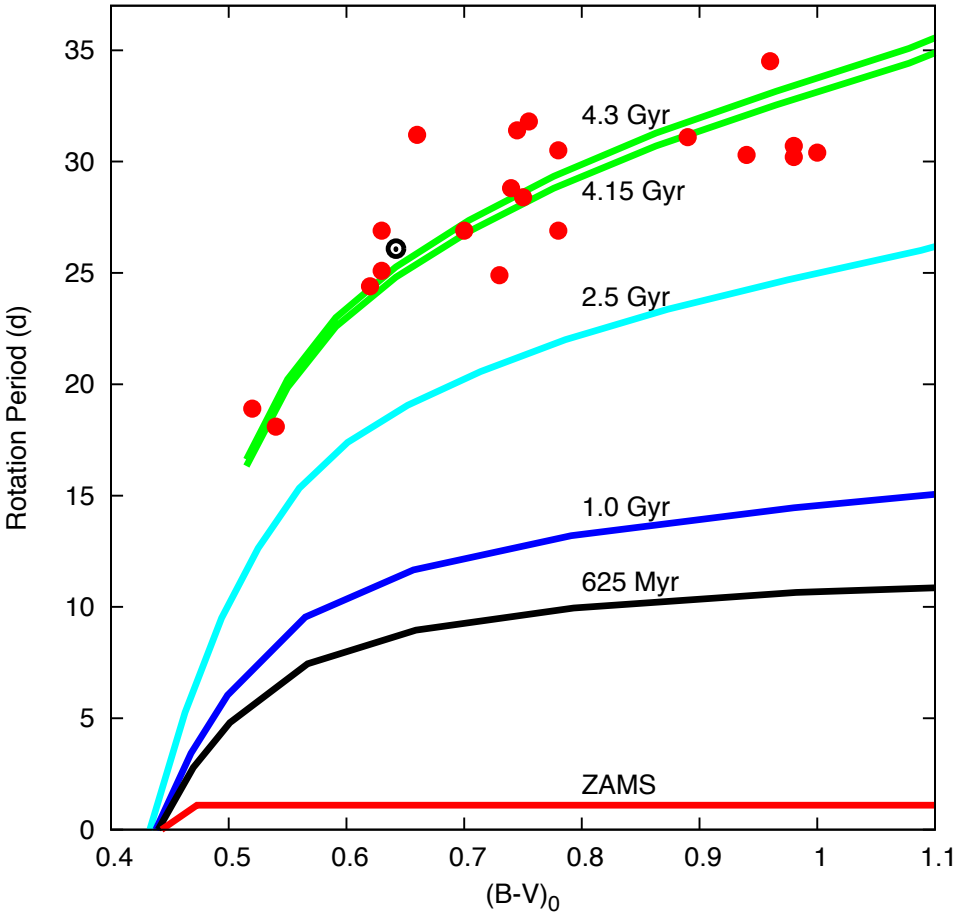

Wide binaries = smallest OCs

B07

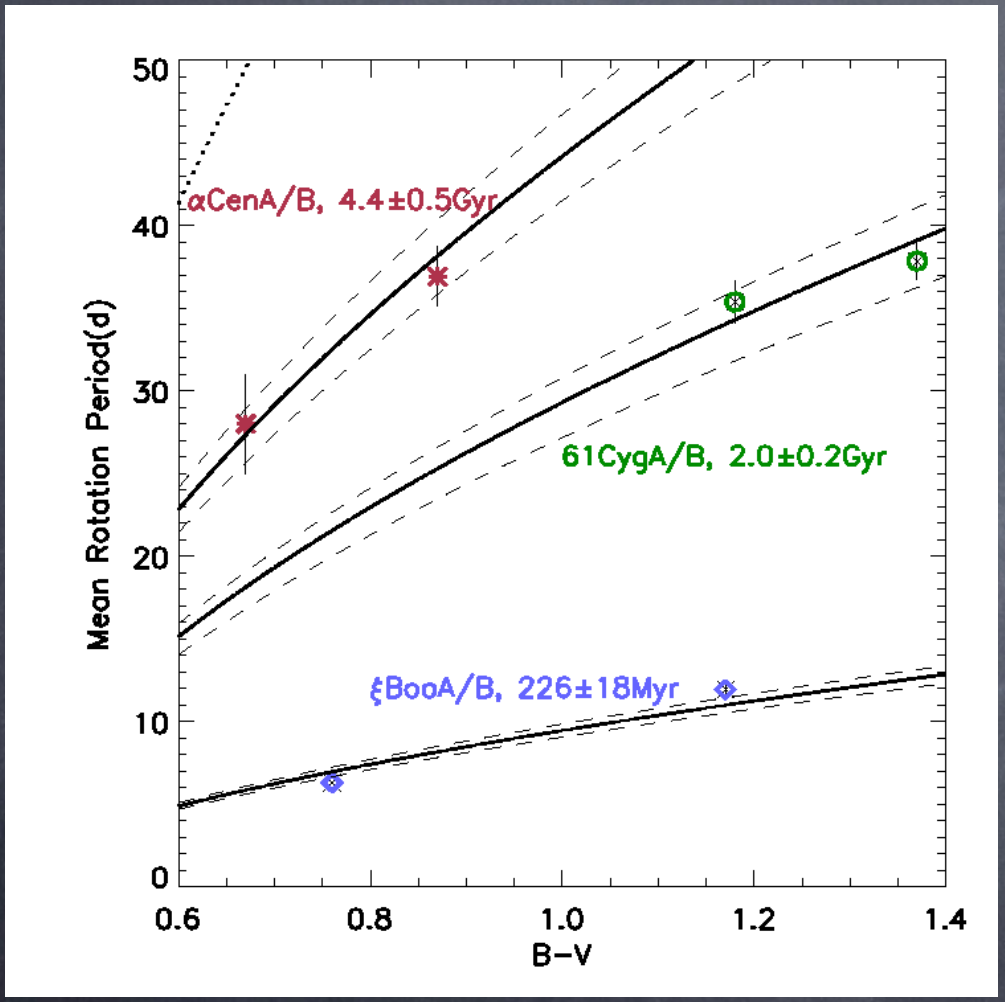

Janes2017

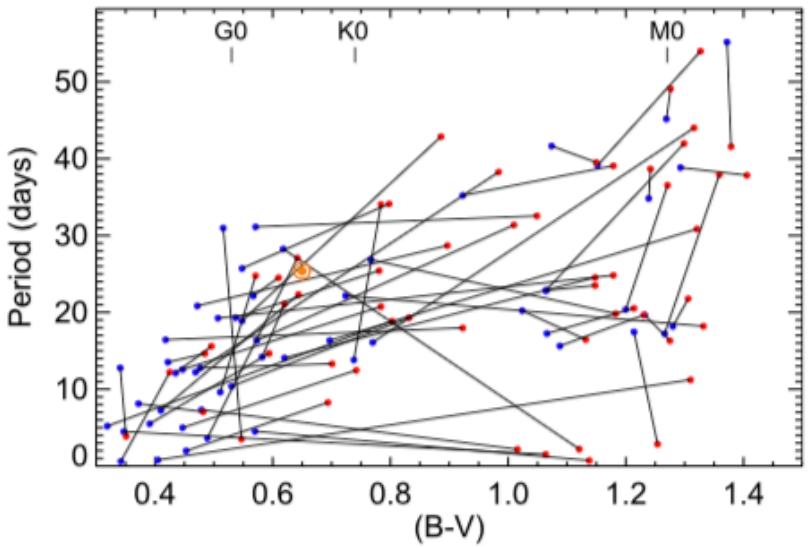

Figure 11. Period–color diagram for CPM pairs with two active components. The lines connect the hotter star of each pair (blue symbols) with the cooler star (red symbol). The $(B - V)$ values are derived from Equation (5). The Sun's position is shown with a dotted circle. The approximate locations of selected spectral types from Table 5 of Kraus & Hillenbrand (2007) are also shown. The blue component of one active pair (number 80) lies outside the diagram so that pair is not shown.

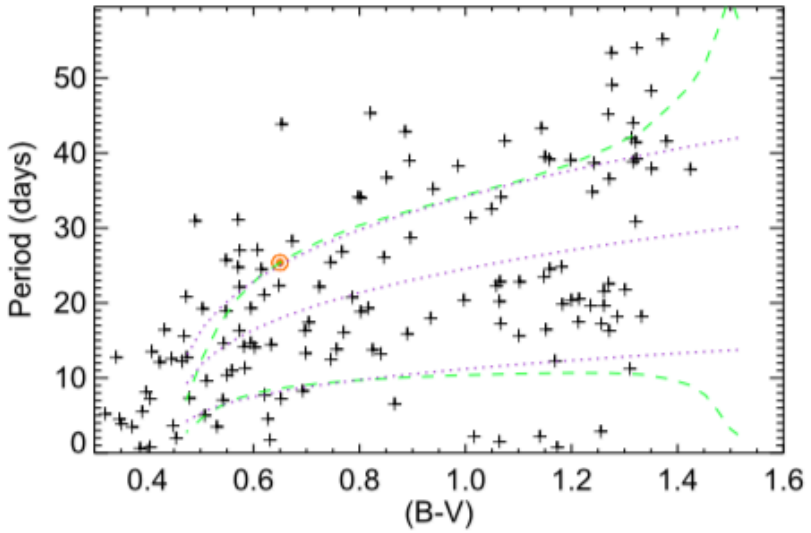

Figure 12. Period–color diagram for all active stars with reliable periods. The Sun's position is shown with a dotted circle. Period–color isochrones are shown for 4.57, 2.5 Gyr, and 600 Myr stars. The green lines are from Barnes (2010) and the purple lines are from Angus et al. (2015). The upper two lines are the 4.57 gyr isochrones. The purple dotted line at intermediate periods represents a 2.5 Gyr isochrone from Angus et al. (2015).

Anomalous braking issue: clusters

van Saders+2016

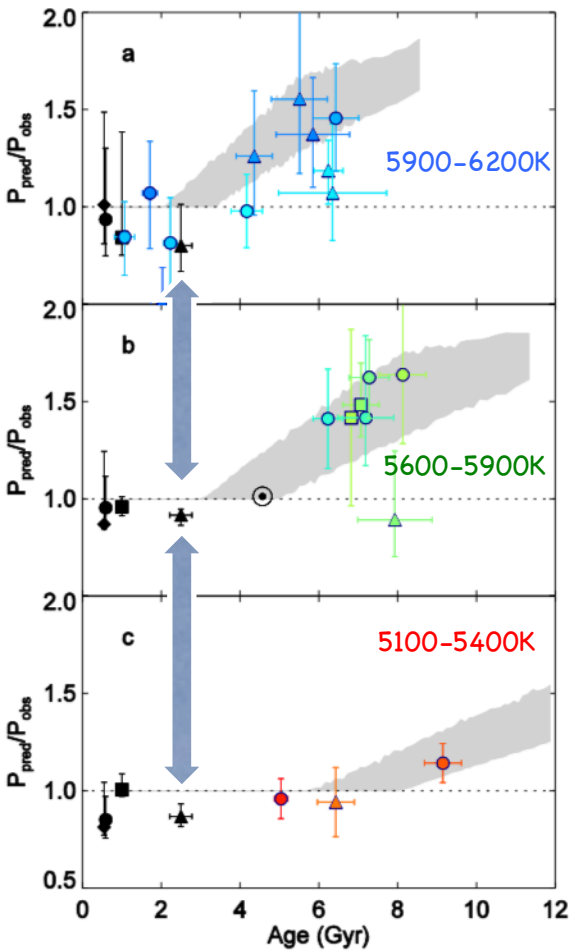

Figure 2 | The ratio of the predicted rotation period[14] to the observed period. Stars are divided into panels of decreasing AMP ZAMS T_{eff} (a. 5900-6200 K, b. 5600-5900 K, c. 5100-5400 K). Period ratios for open clusters are shown as black symbols: M37 (diamond), Praesepe (circle), NGC6811 (square), NGC6819 (triangle). The Sun (⊙) is marked. Colored circles represent seismic targets, colored triangles known planet hosts, and colored squares 16 Cyg A & B. All errors are 1σ. Stars are colored by ZAMS T_{eff}, with blue representing hotter stars. Shaded regions represent the period ratios permitted in each T_{eff} bin for a $Ro_{crit} = 2.16$ model.

NGC 6819 (2.5 Gyr) measured periods vs. 4 models

Meibom+2015

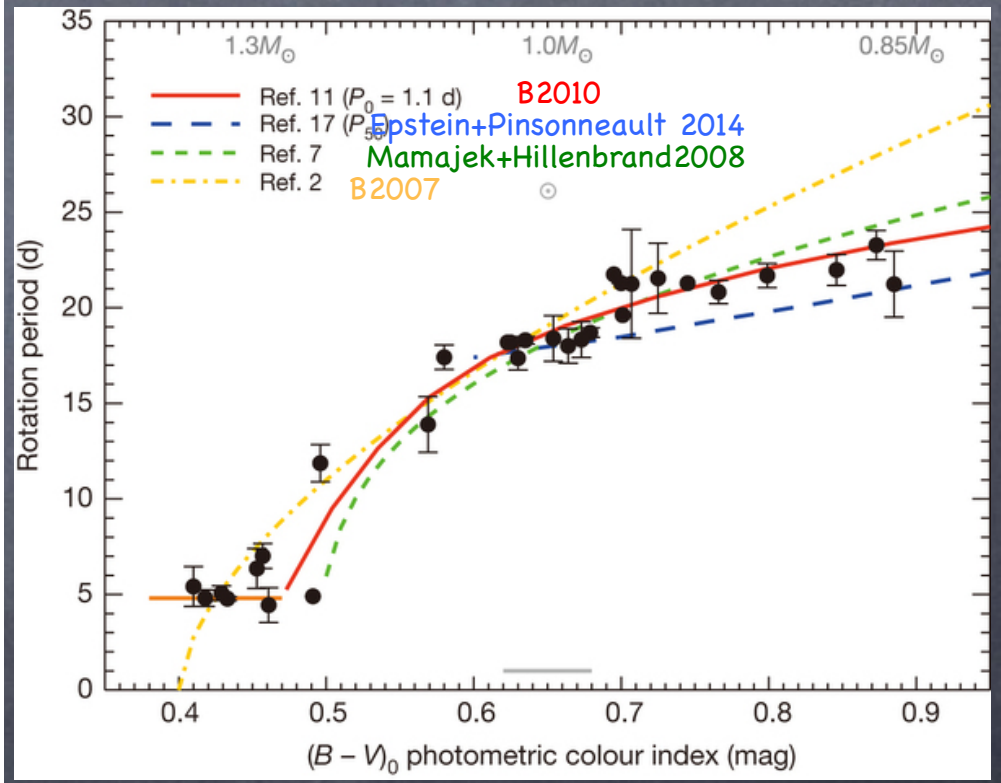

M67 (4.2 Gyr)

B+2016

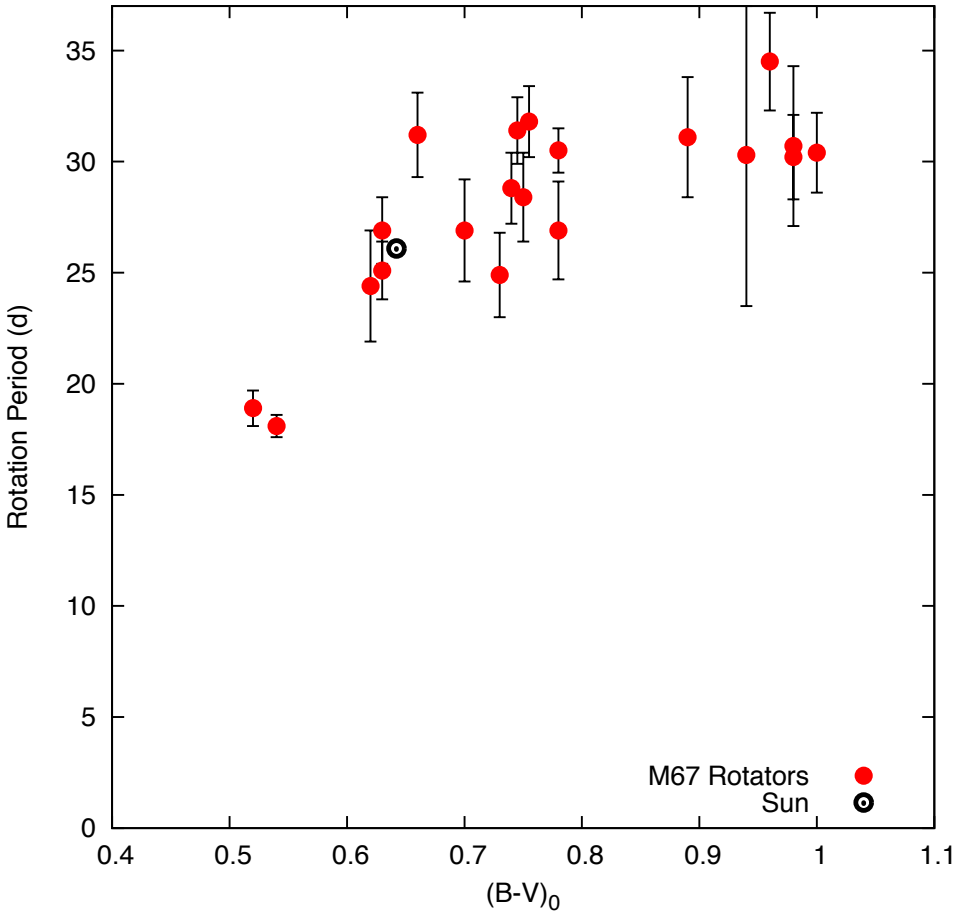

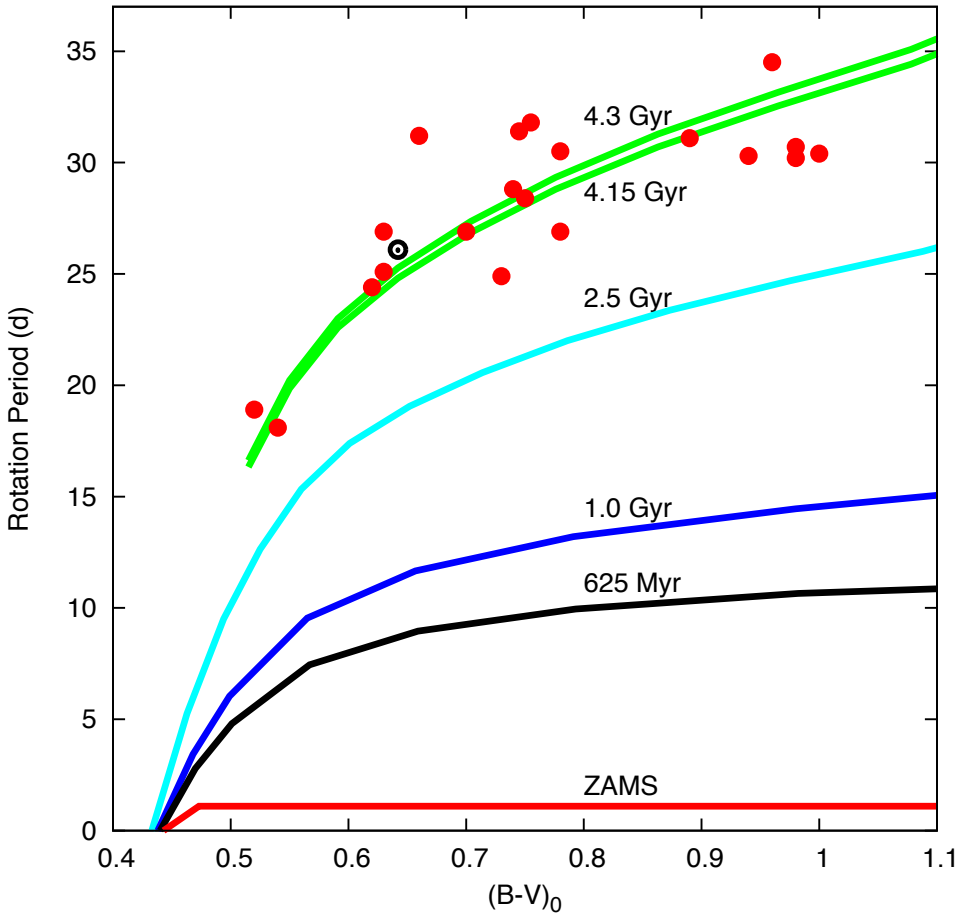

Period change for a sun-like star with age (c.f. Skumanich 1972)

BSW16

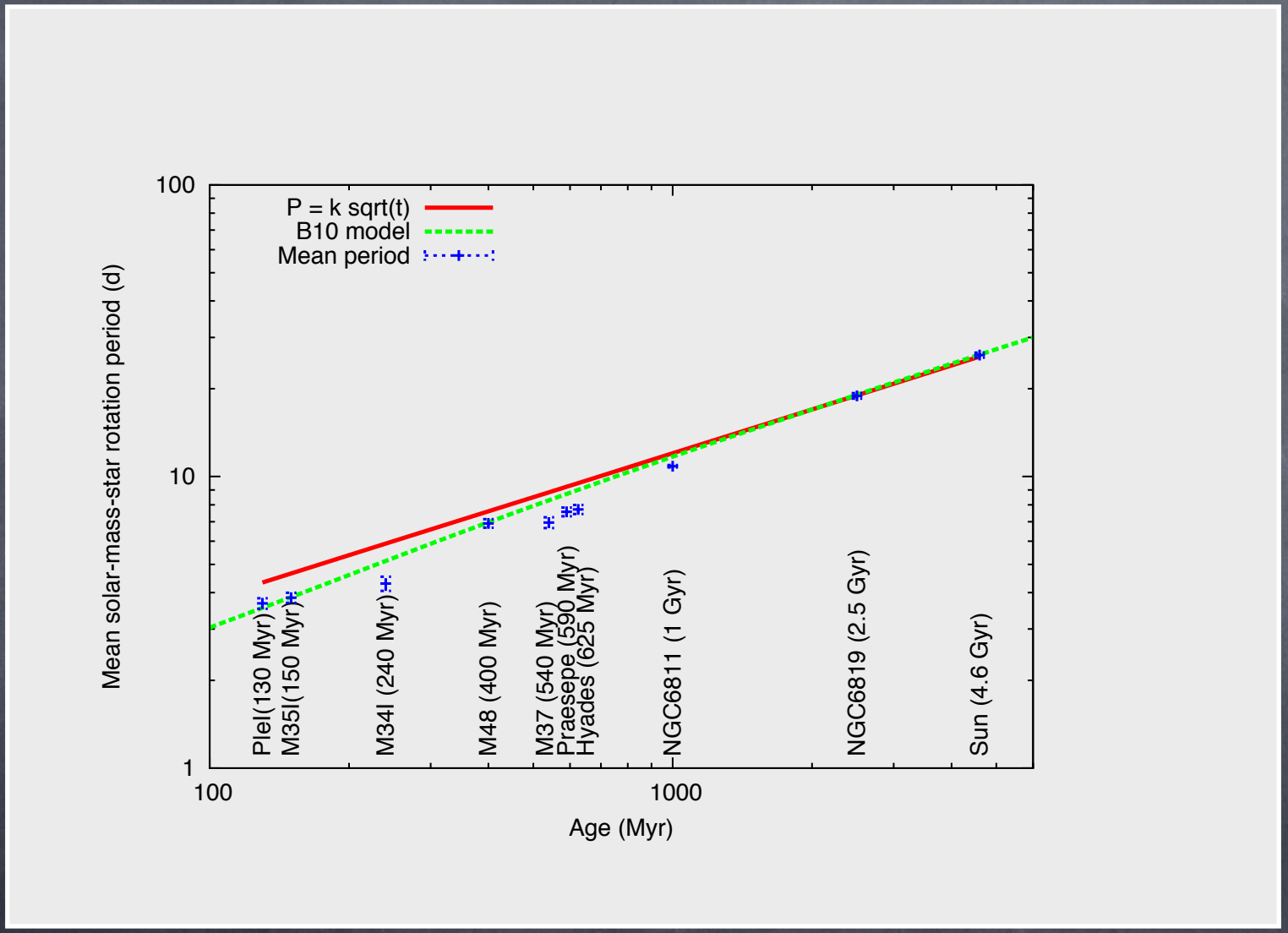

P

t

Anomalous braking issue: field stars

van Saders+2016

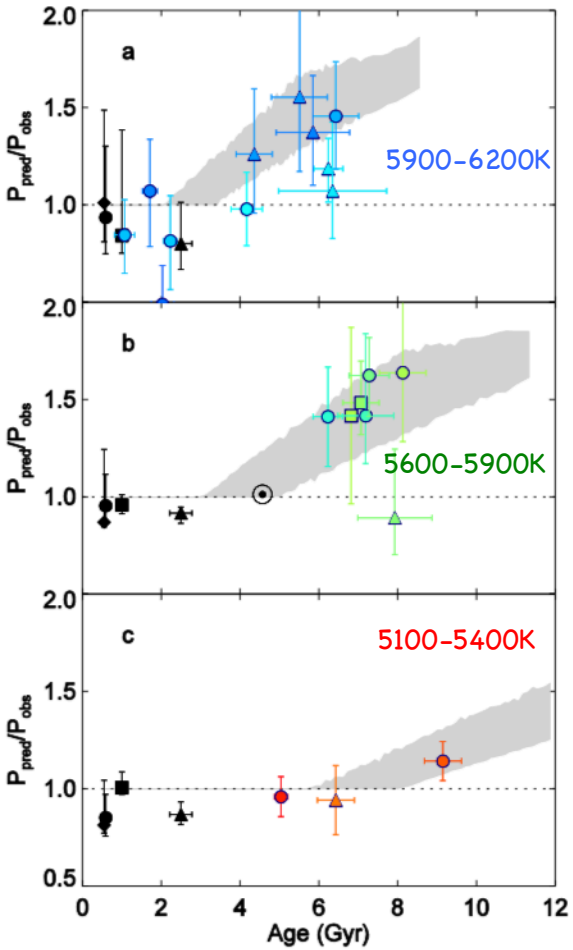

Figure 2 | The ratio of the predicted rotation period[14] to the observed period. Stars are divided into panels of decreasing AMP ZAMS T_{eff} (a. 5900-6200 K, b. 5600-5900 K, c. 5100-5400 K). Period ratios for open clusters are shown as black symbols: M37 (diamond), Praesepe (circle), NGC6811 (square), NGC6819 (triangle). The Sun (⊙) is marked. Colored circles represent seismic targets, colored triangles known planet hosts, and colored squares 16 Cyg A & B. All errors are 1σ. Stars are colored by ZAMS T_{eff}, with blue representing hotter stars. Shaded regions represent the period ratios permitted in each T_{eff} bin for a $Ro_{crit} = 2.16$ model.

Comparison of the 8 van Saders+2016 stars with log g > 4.3, and with 4 metal-poor stars removed

B, Spada, Weingrill 2016

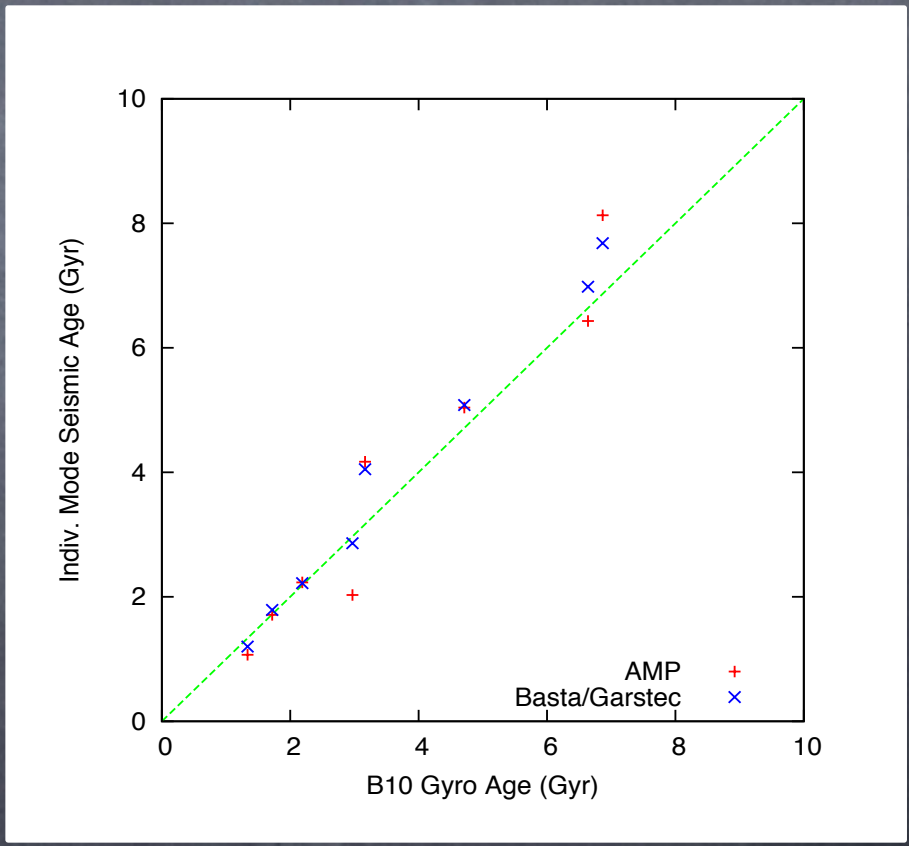

Kepler field star rotation periods

(147,000 periods already in GAIA DR2, and even more from TESS)

Periods from Reinhold+2013

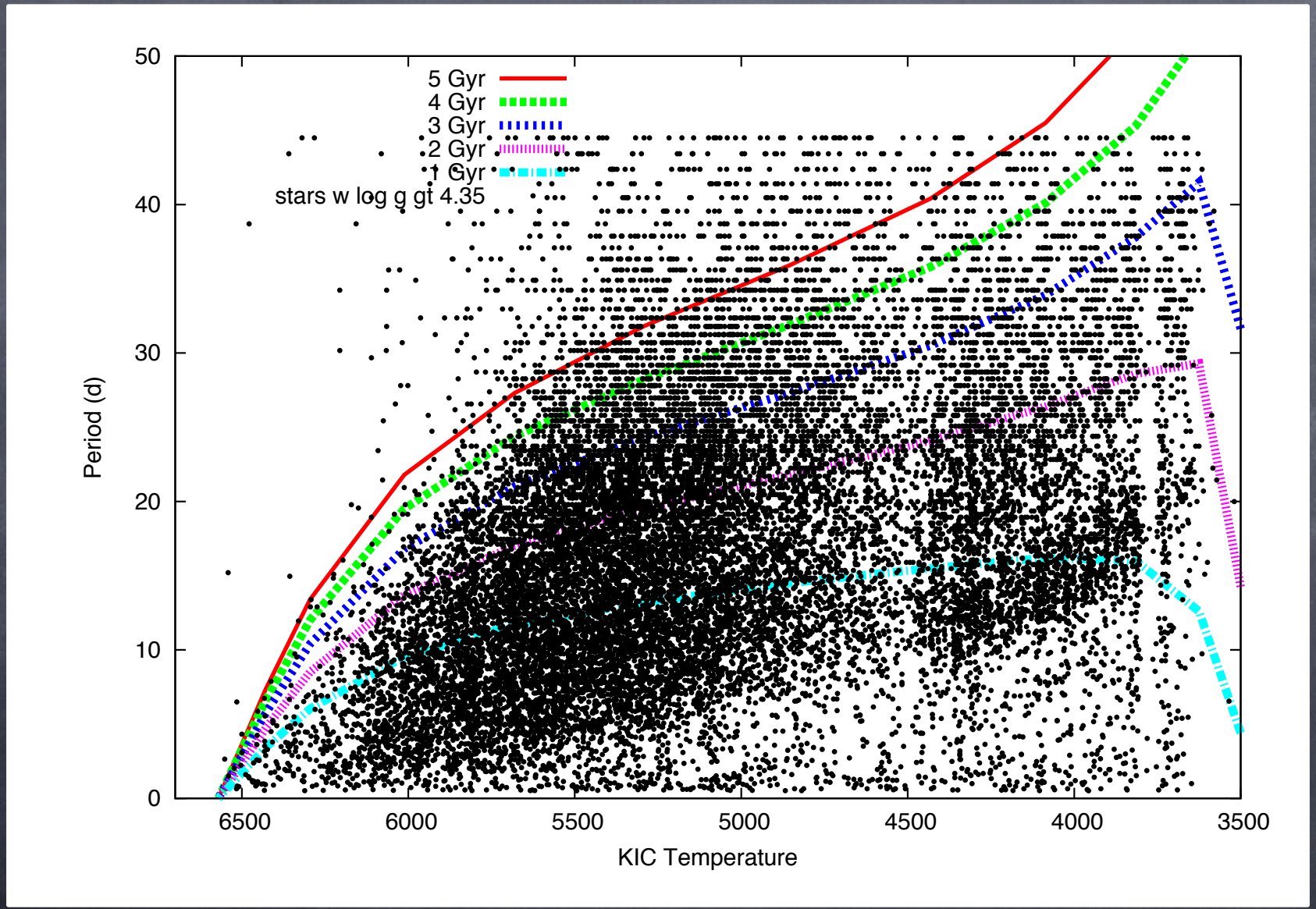

Kepler field star rotation periods

Periods from Reinhold+2013

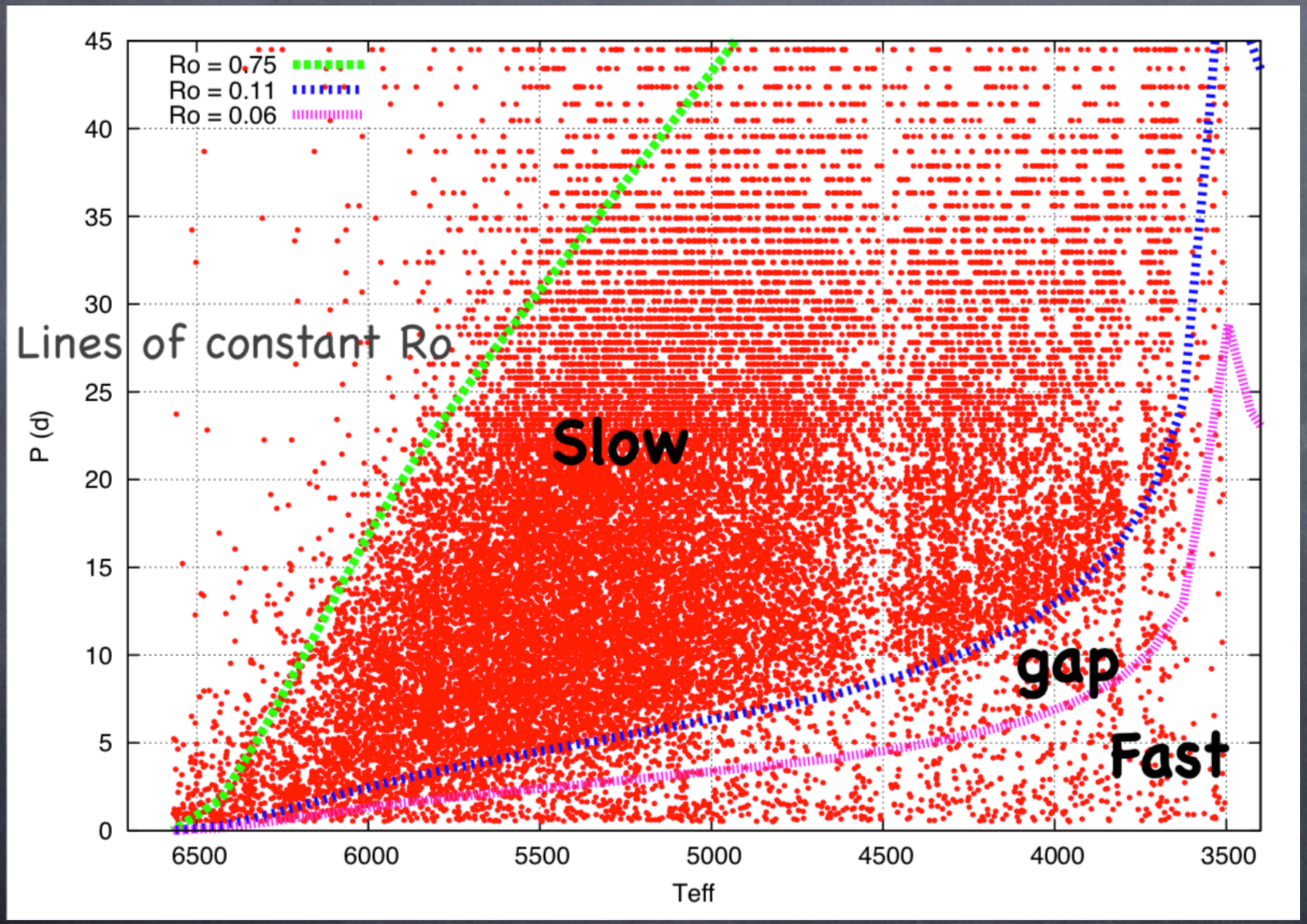

Comparison with chromospheric ages (MW stars: Baliunas+1996)

B07

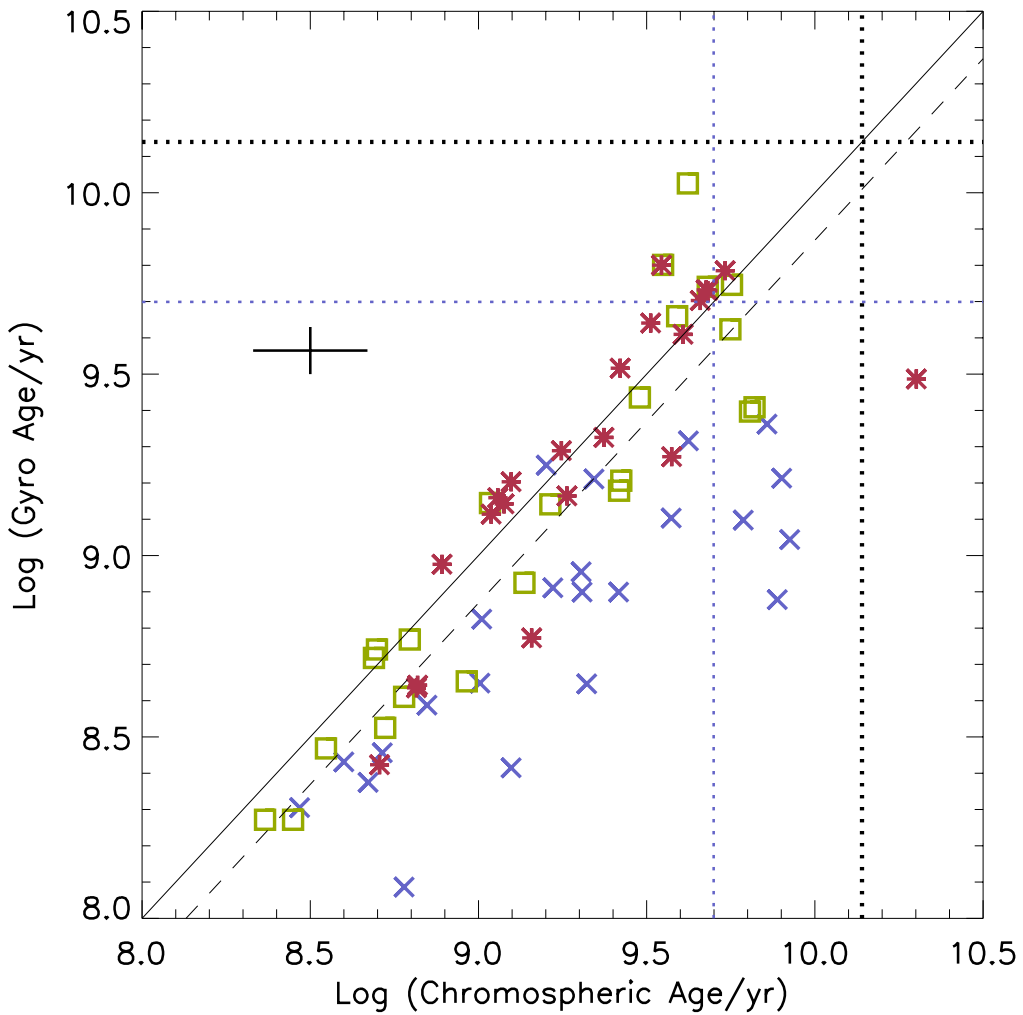

Prognosis

- Activity indicators potentially provide independent ages for many PLATO stars
- Ancillary work is helpful in identifying pathological objects
- Rotation periods are automatically encoded in transit data, and could provide ages for many cool stars, including relatively faint ones; TESS data could be a better test-bed for PLATO than Kepler
- More care is needed with gyrochronology than is sometimes believed to be the case, and more experience/development is needed for older/lower mass/non-solar metallicity stars
- Chromospheric ages are less time-consuming, but a path towards large-scale spectroscopy is unclear; X-Rays (eRosita) might be more feasible
- Benchmarks for both chromospheric and gyro ages could include available open clusters and wide binaries

Extra slides

Cool MS rotators should lie on a P-m-t surface

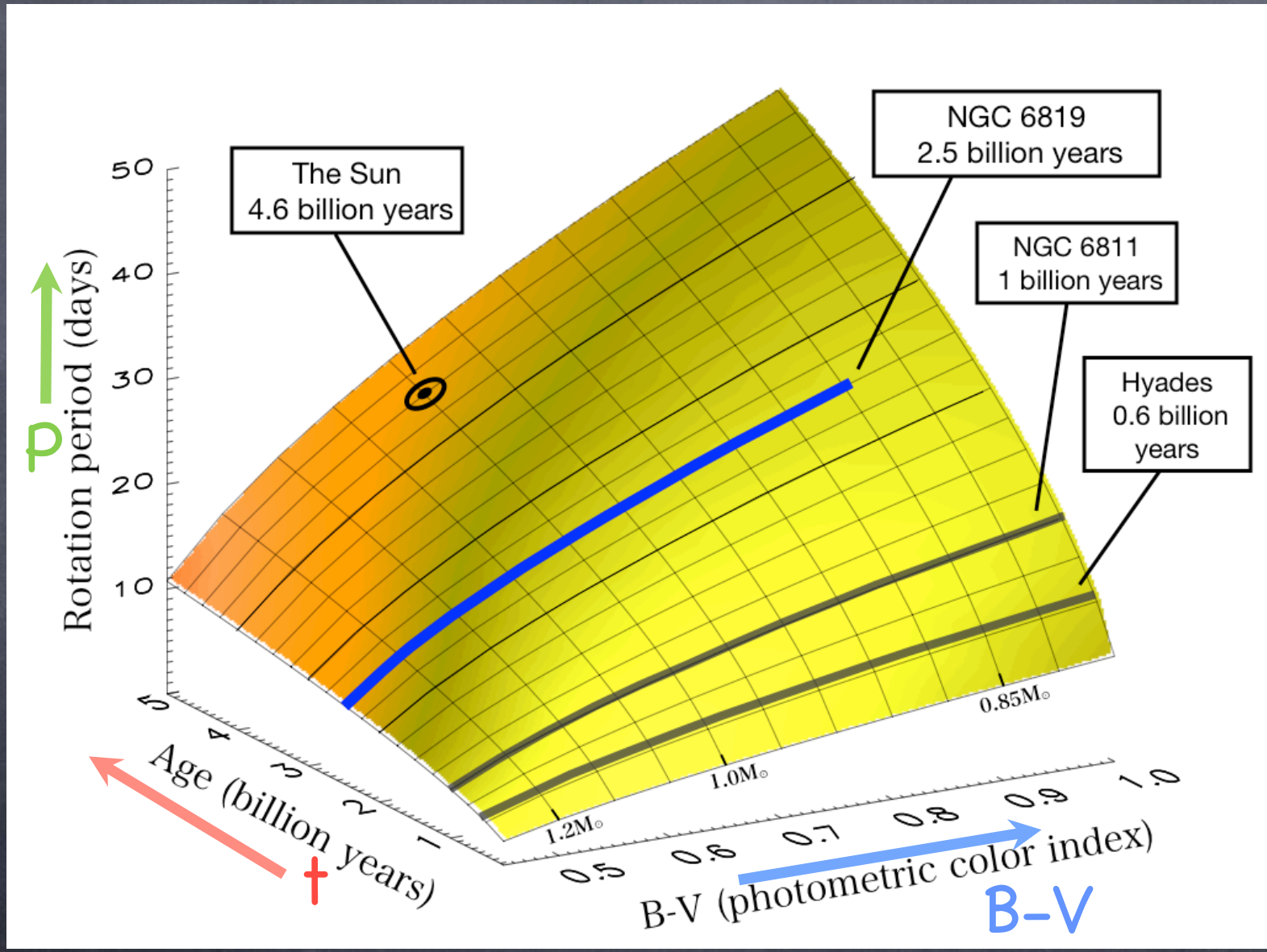

L changes by 2-3x on MS; P changes by 50-100x

L requires distance

L

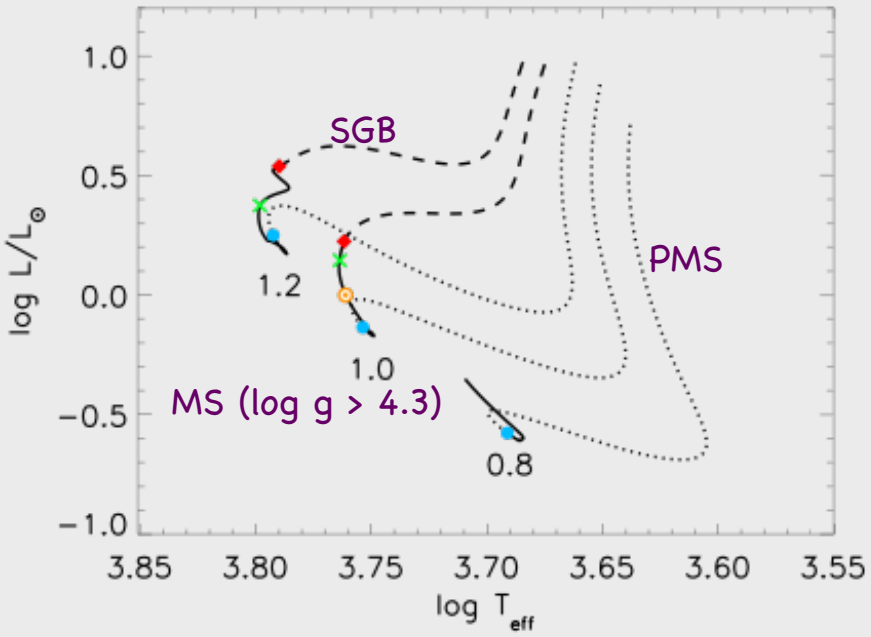

P is distance-independent

P

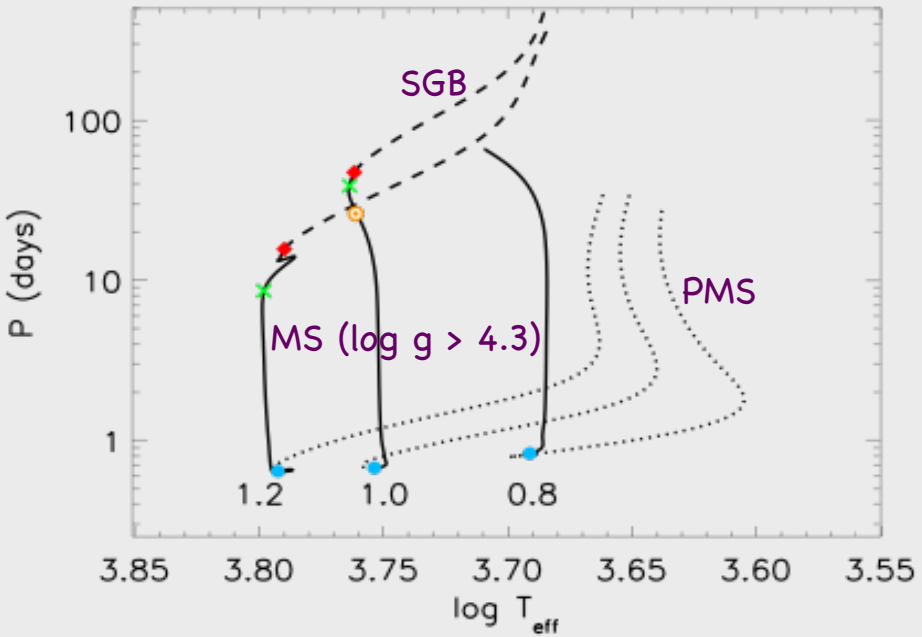

(B+Spada+Weingrill 2016)

Dendrochronology

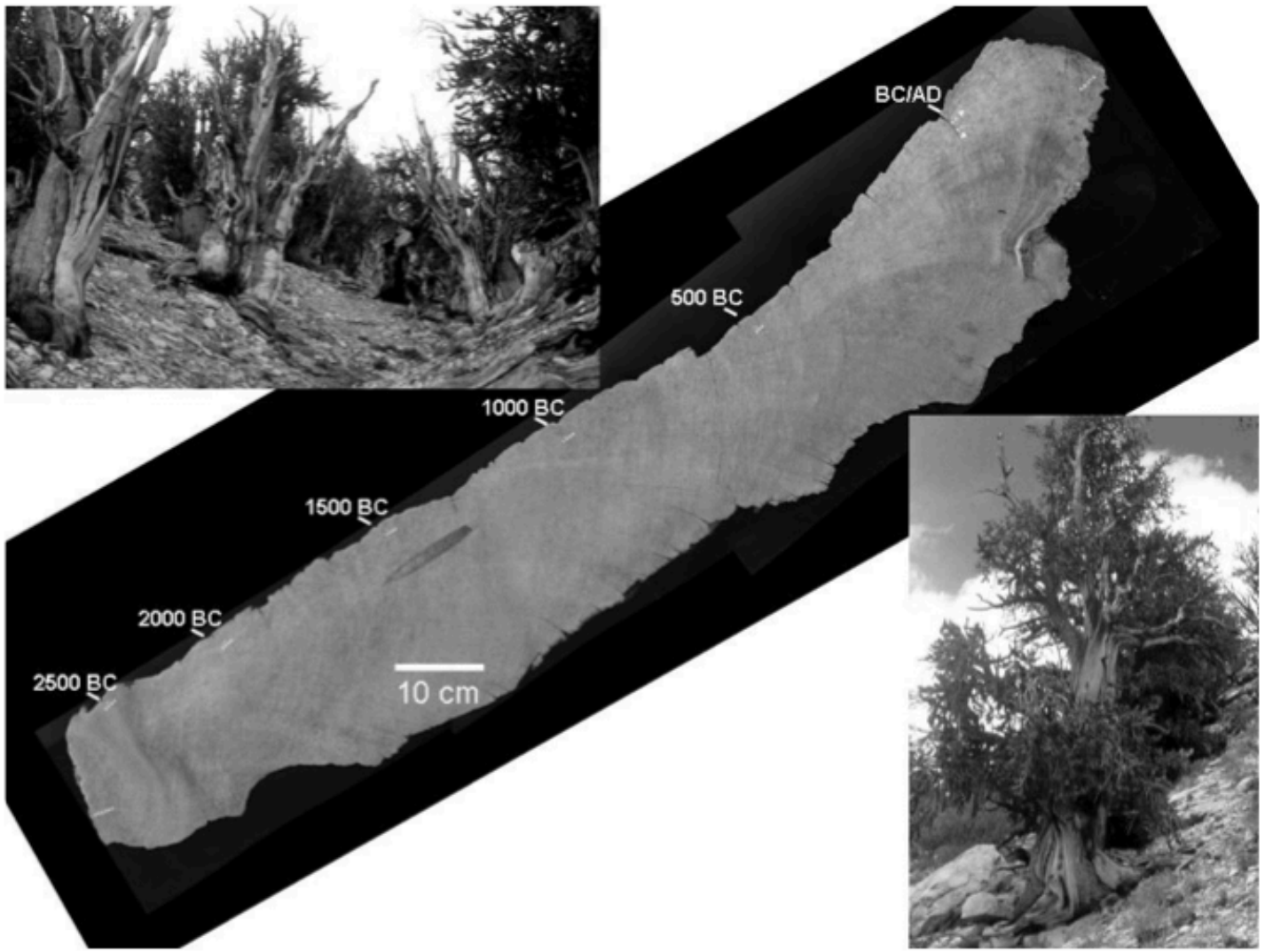

Figure 5 Bristlecone pine cross-section containing ~2700 rings (2963 BC to AD 279), and field photos of bristlecone pines (from the Methuselah Walk area in the California White Mountains) showing circumstances of growth (bark and leaves) on one side of the tree known as "strip-bark."

(Leavitt & Bannister, 2009, Radiocarbon, 51, 373)

M67 (4.2 Gyr)

B+2016

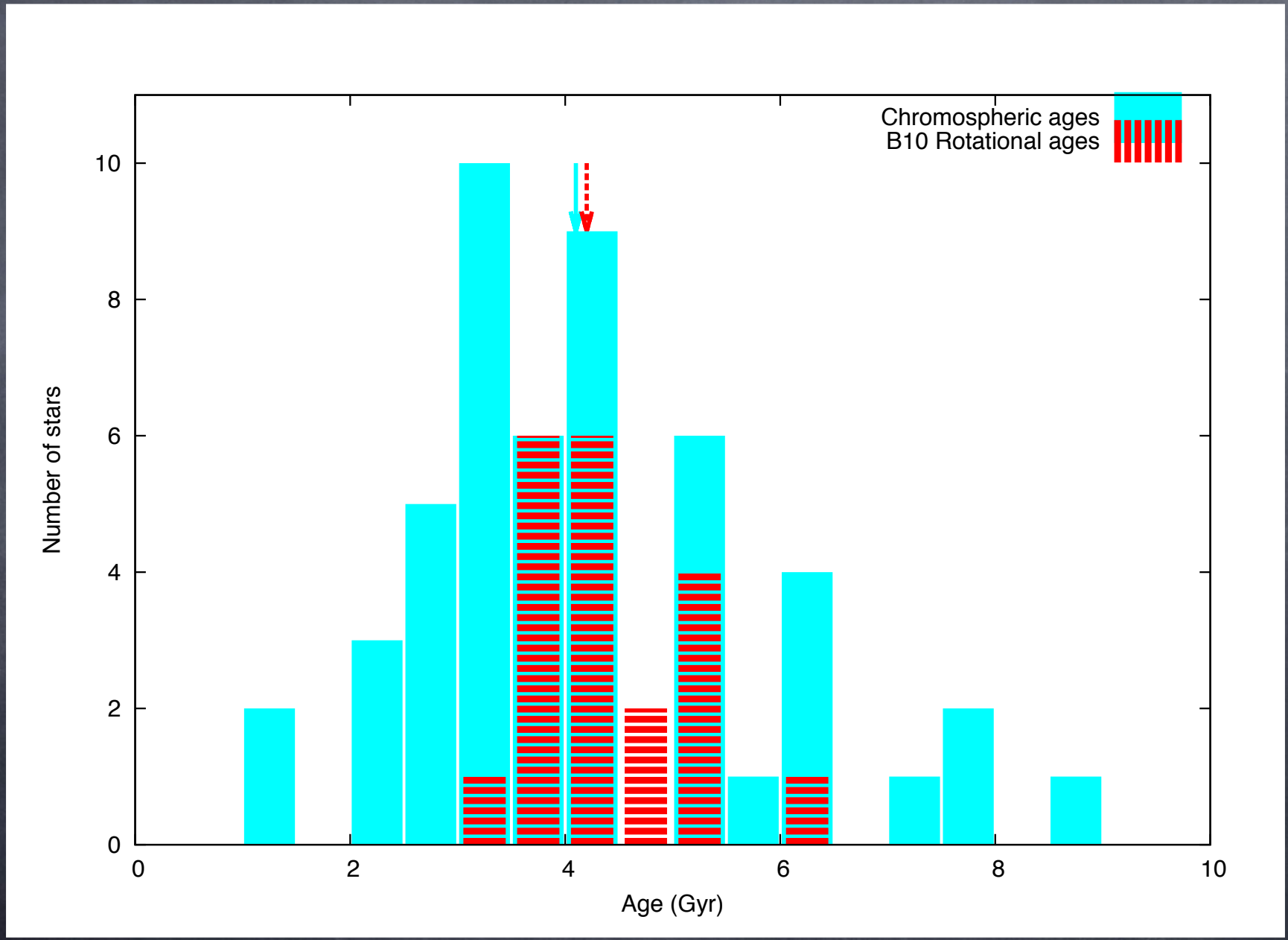

Deacon+2016 (adapted)

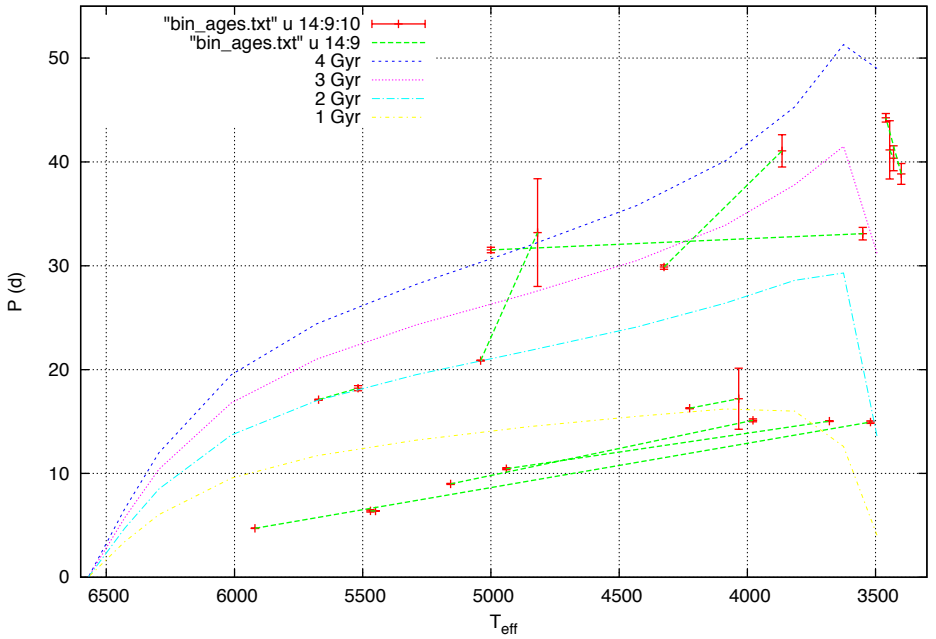

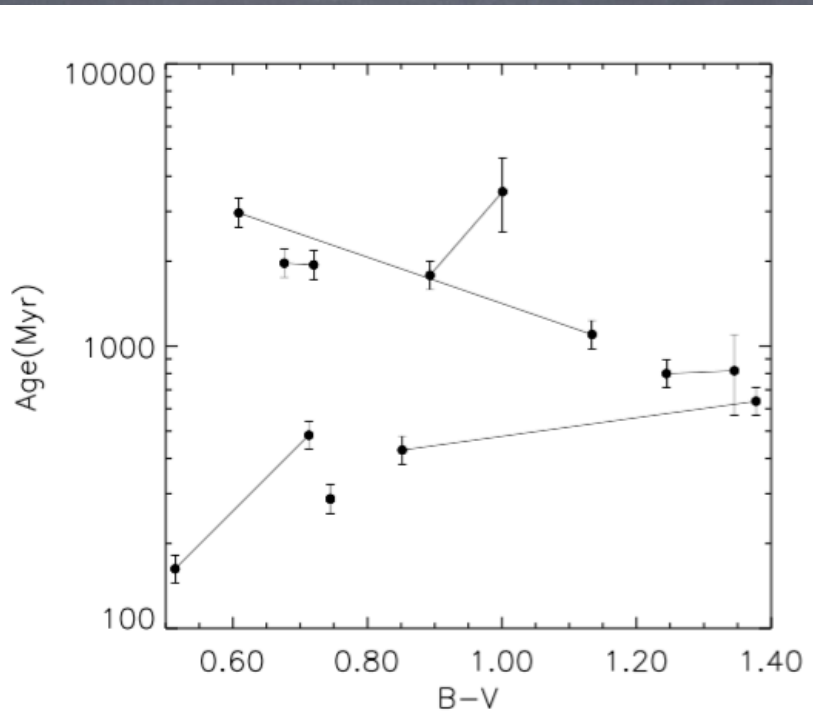

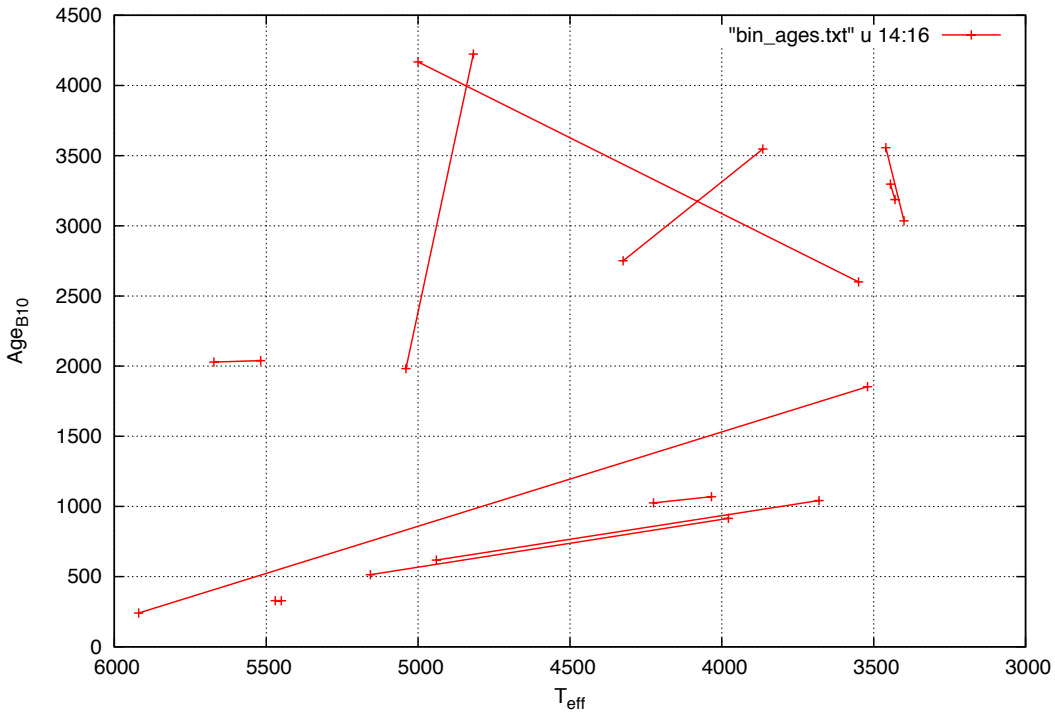

Simplest in P-tau plane

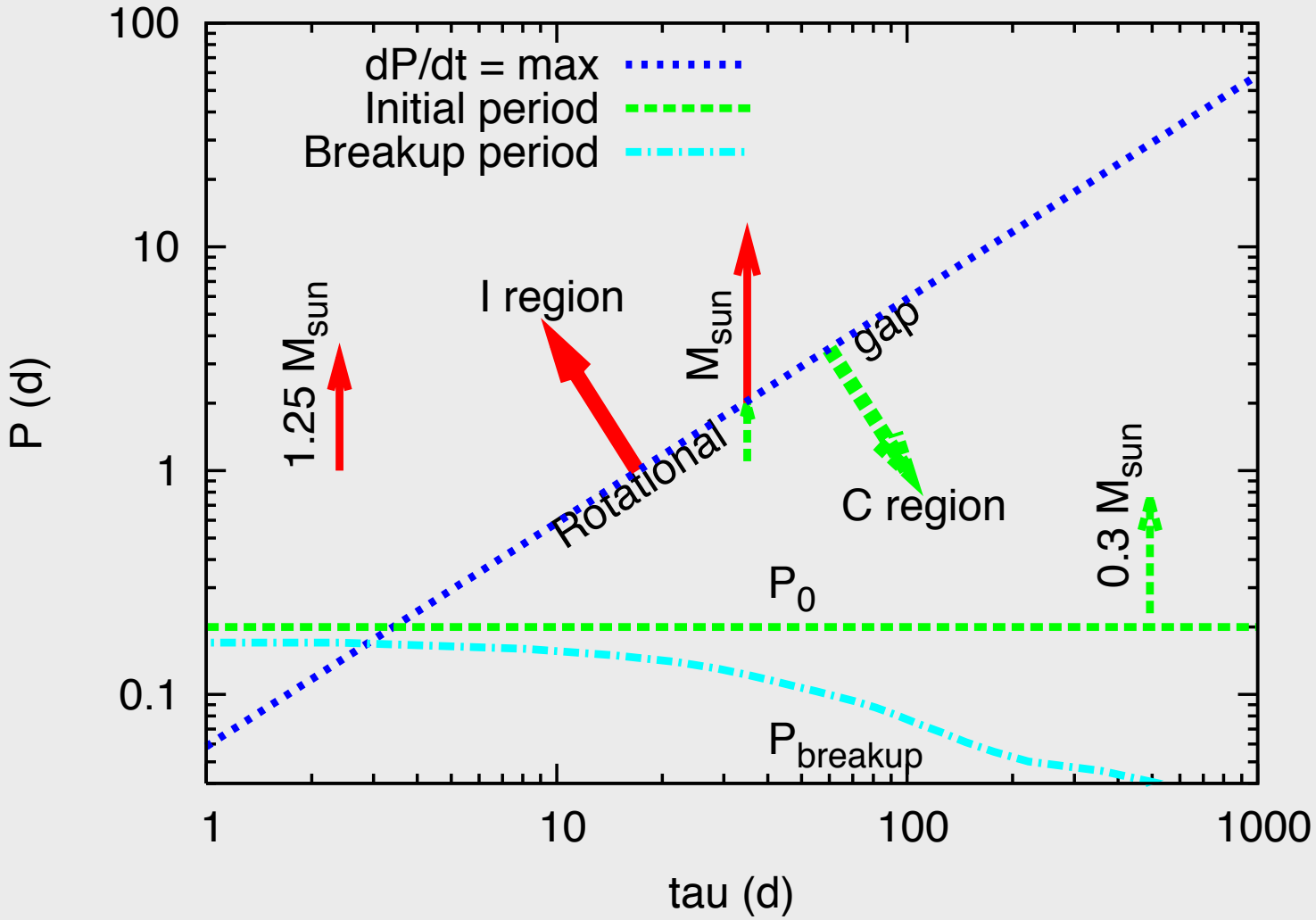

Comparison with B2010 model

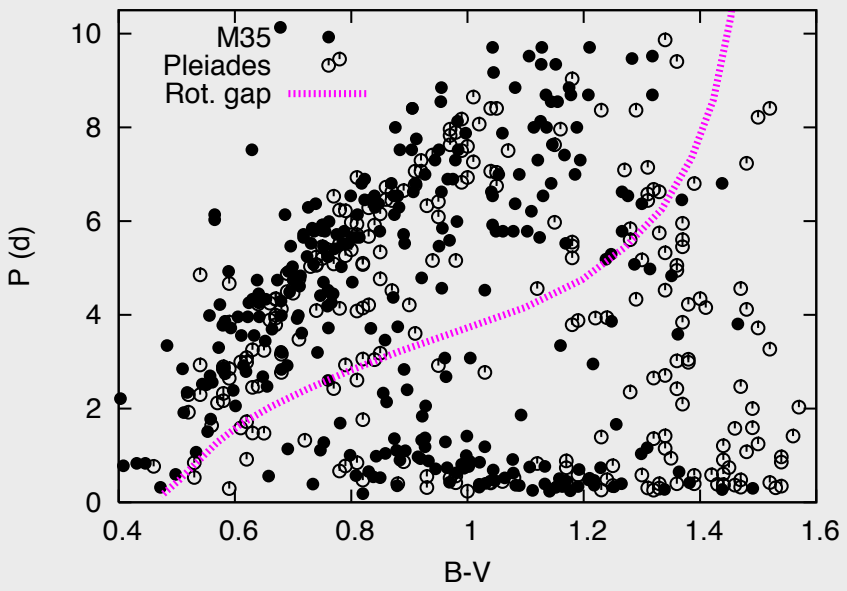

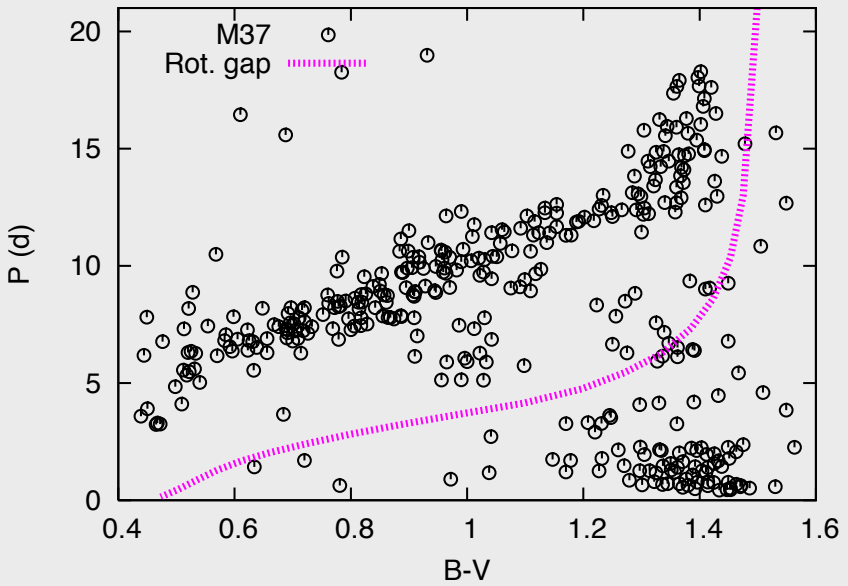

B2010 model: dP/dt = dP/dt (tau)